


CARBON FIBER COMPOSITES AND COMPOUNDS INTERCEPTING ENERGETIC
PROTON BEAMS – IRRADIATION DAMAGE AND THERMAL SHOCK

N. Simos¹, Z. Zhong¹, H. Kirk, L-P Trung, K. McDonald³, Z. Kotsina⁵, P. Nocera⁶

²CERN TEAM (R. Assmann, S. Redaelli, A. Bertarelli, E. Quaranta)

³FERMI Lab (R. Zwaska², K. Amigan², P. Hurh², N. Mokhov)

⁴Princeton University, Princeton, New Jersey, USA

⁵Department of Solid State Physics, National and Kapodistrian University of Athens, Greece

⁶Department of Solid State Physics, University of Rome, Italy

For submission to PRST-AB
Physical Review Special Topics – Accelerators and Beams
(PRST-AB)

 Corresponding author: simos@bnl.gov

CARBON FIBER COMPOSITES AND COMPOUNDS INTERCEPTING ENERGETIC PROTON BEAMS – IRRADIATION DAMAGE AND THERMAL SHOCK

N. Simos¹, Z. Zhong¹, H. Kirk¹, L-P Trung¹, K. McDonald³, Z. Kotsina⁵, P. Nocera⁶

¹Brookhaven national Laboratory, Upton, NY 11973, USA

²CERN TEAM (R. Assmann, S. Redaelli, A. Bertarelli, E. Quaranta)

³FERMI Lab (R. Zwaska³, K. Amigan³, P. Hurh³, N. Mokhov³)

⁴Princeton University, Princeton, New Jersey, USA

⁵Department of Solid State Physics, National and Kapodistrian University of Athens, Greece

⁶Department of Solid State Physics, University of Rome, Italy

ABSTRACT

A comprehensive study on the effects of energetic protons on carbon fiber composites and compounds under consideration for use as low-Z pion production targets in future high power accelerators and low-impedance collimating elements for intercepting TeV-level protons at the Large Hadron Collider has been undertaken addressing two key areas namely thermal shock absorption and resistance to irradiation damage. Carbon fiber composites of various fiber weaves have been widely used in aerospace industries due to unique combination of high temperature stability, low-density and high strength. The performance of carbon-carbon composites and compounds under intense proton beams and long-term irradiation have been studied in a series of experiments and compared with the performance of graphite. 24 GeV proton beam experiments confirmed the inherent ability of 3D C/C fiber composite to absorb shock. A series of irradiation damage campaigns explored the evolution of the different C/C structures as a function of proton fluence and irradiating environment. The studies confirmed the influence of the environment on structural integrity loss with radiolytic oxidation as most pronounced detrimental factor above a threshold proton fluence of $5 \cdot 10^{20}$ pcm⁻². The carbon-fiber composites were shown to exhibit significant anisotropy in their dimensional stability driven by the fiber weave and the microstructural behavior of the fiber and carbon matrix accompanied by the presence of manufacture porosity and defects. Carbon-fiber reinforced compounds exhibited significant decrease in post-irradiation deformation even after low dose levels and high degree of structural degradation at fluence $\sim 5 \cdot 10^{20}$ pcm⁻² while irradiated in vacuum and at higher temperature.

Finally, X-ray diffraction studies on irradiated C/C composites and carbon-fiber reinforced Mo-graphite compound revealed (a) low graphitization in the as-received 3D C/C and high graphitization in the MoGRCF compound (b) irradiation-induced graphitization of least crystallized phases in the carbon fibers accompanied by increased inter-planar distances along the c-axis of the graphite crystal with increasing fluence and coalescence of interstitial clusters to new crystalline planes between basal planes.

KEYWORDS: *Irradiation damage, high temperature annealing, oxidation, x-ray diffraction, carbon fiber composite, molybdenum-graphite metal matrix*

Corresponding Author: simos@bnl.gov

1 Introduction

Planned next generation, multi-MW power accelerators will require high-performance and high reliability secondary particle production targets to generate intense neutrino and other rare particle beams. Towards this end the understanding of the behavior of target materials under extreme states of long term irradiation combined with thermal shock must greatly expand to remain in step with the order of magnitude increase in the demand. Primary concerns are (a) the anticipated accumulation of radiation damage in the materials of choice and the resulting changes in their physio-mechanical properties and (b) the ability of materials to withstand intense beam-induced thermal shock while their physical properties are continuously undergoing changes. In target-like applications such as the collimating structures of the 7 TeV proton beam at the LHC where the selected material intercepts the beam halo, extreme dimensional stability and resilience to structural degradation is required.

C/C composites consisting primarily by a carbon matrix reinforced with carbon fibers in 1-D, 2-D and 3-D weave manner have enjoyed applications in a number of industries, such as aerospace owed to their excellent thermal shock resistance, high specific strength and modulus of elasticity. Their superior thermal resistance and their ability to maintain strength at elevated temperatures has introduced them to applications with severe thermal conditions such as the space shuttle re-entry where they have been utilized as a protective thermal shield. Serious consideration of these composites for application in very high temperature reactors (VHTR) and fusion reactors has been given due to the added properties of high sublimation temperature (~ 3600 K), high thermal conductivity and low neutron absorption cross section.

Studies at elevated temperatures of C/C aiming to understand the microstructural evolution of the complex structure of these composites with and in the absence of irradiating environments have been conducted. The microstructural evolutions of three-dimensional carbon-carbon composite materials irradiated by carbon ions at elevated temperatures were studied by S-C Tsai and co-workers [1] concluding that the composite exhibits lower degree of graphitization than nuclear graphite and that modest irradiation levels of $7.0 \cdot 10^{21} \text{ C}^+/\text{m}^2$ at temperatures of 600°C led to observable radiation damage in the form of distinct cracks and grain distortions in the matrix as well as braking of fibers. The structural modifications of carbon-carbon composites under high temperature and ion irradiation (2 keV hydrogen of low flux $5 \cdot 10^{16} \text{ ions m}^{-2} \text{ s}^{-1}$) were addressed by T. Paulmier and co-workers [2]. Their study revealed that the microstructure of the as-received carbon-carbon is strongly influenced by the processing route and that 2D C/C structures exhibit increased disorder with elevated temperatures. No influence of irradiation at elevated temperatures could be observed due to low energy and flux.

Irradiation-induced structure and property changes in C-C composites for use in Tokamak plasma-facing was studied by T. Burchell [3]. Results of two irradiation experiments of 1-D, 2-D and 3-D carbon-composite structures irradiated at the High Flux isotope Reactor (HIFR) were reported. The study results indicated that the 3D C/C structure behaves more isotopically than two-directional or unidirectional composites and that the thermal conductivity, while severely degraded by neutron irradiation can partially recover through annealing. The effects of carbon fiber orientation and graphitization on solid state bonding of C/C Composite to nickel were studied by Ishida [4]. Specifically, C/C composites with the two types of carbon fiber orientations, which are heat-treated at two different temperatures, were used and the influences of both fiber orientation and graphitization on the joining of C/C composites to metals were investigated. Load-displacement tests were conducted revealing that the longitudinal section of carbon fiber undergoes slip deformation due to crystallographic anisotropy. Direct comparison of load-deflection data with results from the present study will be made later in the text. In [5] composite materials that include C/C composites and SiC/SiC in extreme radiation and temperatures for application in next generation high temperature reactors are discussed. Relevant to the behavior of C/C composites are

studies conducted and reporting on nuclear graphite focusing on the microstructural and physical property evolution as a function of temperature and fluence^[5, 6, 7, 8, 9, 10, 11].

In an effort to study the effects of energetic protons on carbon fiber composites and compounds under consideration for use as low-Z pion production targets in future high power accelerators and low-impedance collimating elements for intercepting TeV-level protons at the Large Hadron Collider a multi-faceted study has been undertaken addressing two key areas namely thermal shock absorption and resistance to proton irradiation damage. The experimental study sought to evaluate the performance of carbon-carbon composites and compounds under intense proton beams and long-term irradiation have and compare it with neutron data as well as with the performance of graphite.

To address shock absorption 24 GeV tight proton beams were used in experiments to confirm the inherent ability of 3D C/C fiber composite to absorb shock^[12, 13, 14, 15]. This was conducted at the BNL Accelerator Gradient Synchrotron (AGS). Experimental data on the dynamic response of 3D C/C composite and graphite for comparison are presented and discussed in this paper

Following the beam shock experiment a series of irradiation damage campaigns were launched exploring the evolution of the different C/C structures as a function of proton fluence and irradiating environment. The studies confirmed the influence of the environment on structural integrity loss with radiolytic oxidation as most pronounced detrimental factor above a threshold proton fluence of $5 \cdot 10^{20}$ pcm⁻². The carbon-fiber composites were shown to exhibit significant anisotropy in their dimensional stability driven by the fiber weave and the microstructural behavior of the fiber and carbon matrix accompanied by the presence of manufacture porosity and defects. Carbon-fiber reinforced compounds exhibited significant decrease in post-irradiation deformation even after low dose levels and high degree of structural degradation at fluence $\sim 5 \cdot 10^{20}$ pcm⁻² while irradiated in vacuum and at higher temperature. The detail experimental data of dimensional stability and strength on 2D C/C, 3D C/C composites and Mo-GRCF compound are investigated and reported.

X-ray diffraction studies on irradiated C/C composites and carbon-fiber reinforced Mo-graphite compound were conducted using high energy polychromatic and monochromatic beams (200 keV and 70 keV respectively) at the BNL Synchrotron (NSLS). The studies focused on the effects of proton irradiation on the microstructure and the lattice change. They revealed low graphitization in the as-received 3D C/C and high graphitization in the Mo-GRCF compound and irradiation-induced graphitization of least crystallized phases in the carbon fibers.

Experiments were also conducted using high temperature annealing, differential scanning calorimetry (DSC) and scanning electron microscopy (SEM) at the BNL Center of Functional nanomaterials (CFN) in order to characterize the C/C composites and the metal matrix compound Mo-GRCF and study their evolution with temperature. Figure 1 depicts SEM micrographs of the 3D C/C structure indicating the presence of manufacture defects and cracks resulting from the differential expansion in fibers and matrix. Figure 2 shows the evolution of the Mo-GRCF metal matrix compound with temperature up to 965°C. The carbon fibers integrated into the metal matrix composite are clearly shown at room temperature while at 400°C a disordered structure is observed. At higher temperatures crystallization of phases is seen.

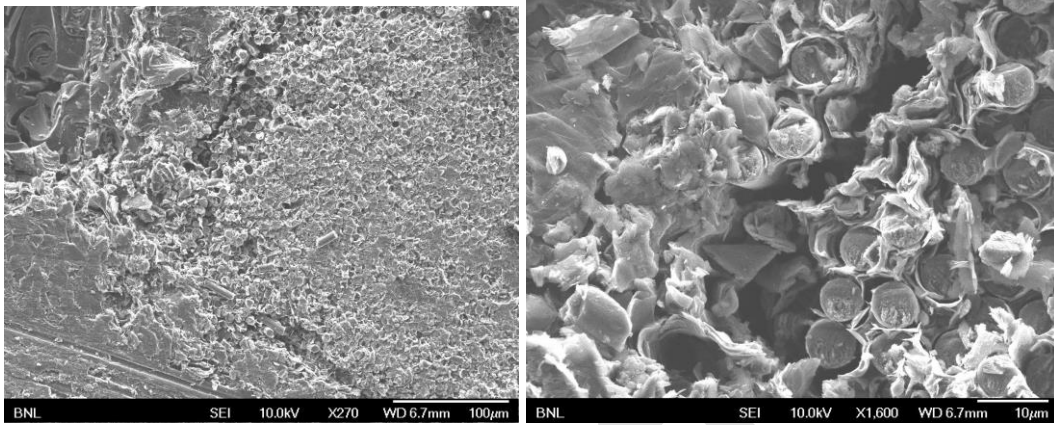


Figure 1: SEM micrographs of 3D C/C composite

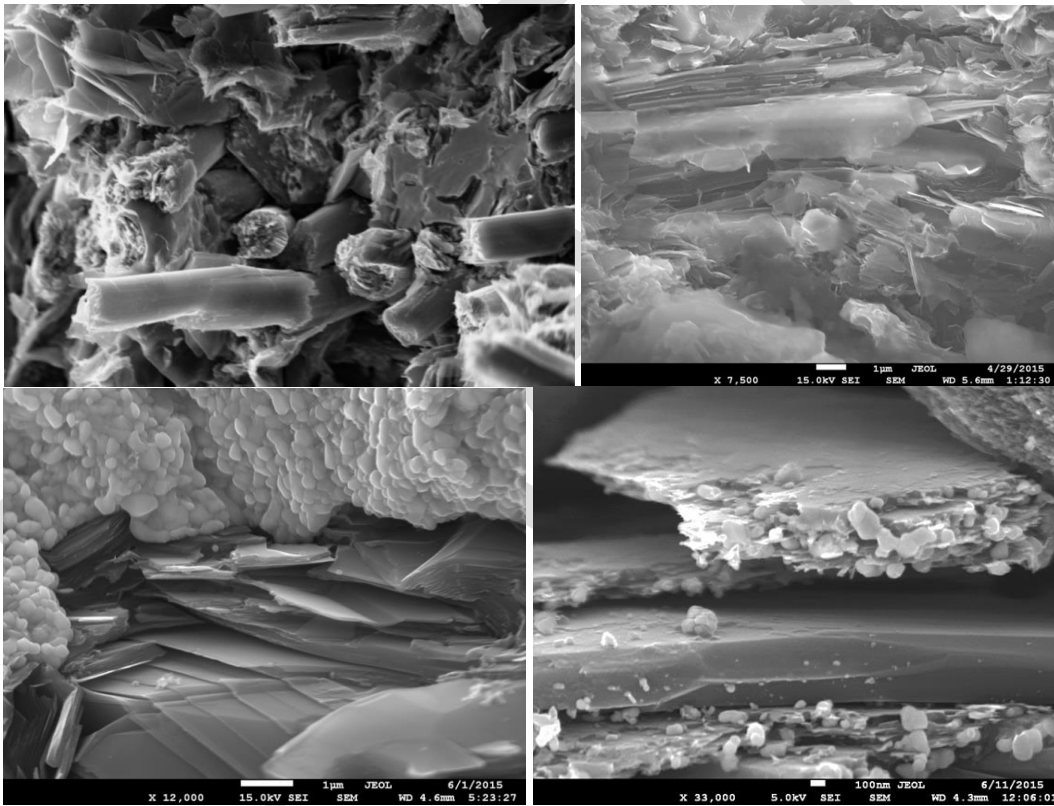


Figure 2: SEM micrographs of MoGRCF with integrated C/C fibres following annealing at elevated temperatures (a=RT, b=400°C, c=720°C, d=965°C). The MoGRCF depicted is characterized by 21.51% and 78.485% carbon atomic fraction respectively.

2. Experimental

The array of experiments focusing on the survivability of C/C composite structures and compounds consisted of beam shock tests and several proton irradiation damage experiments. Specifically,

Under the E-951 BNL experiment 24 GeV proton tight beam pulses of intensity $\sim 3.1 \cdot 10^{12}$ protons/pulse and $\sigma_x = 0.7$ mm, $\sigma_y = 1.7$ mm from the Accelerator Gradient Synchrotron (AGS) were directed on 3D C/C and ATJ graphite cylindrical targets of 1cm radius and 12cm length respectively. The C/C and graphite rod targets were instrumented with Fabry-Perot fiber optic strain gauges capturing the dynamic response due to induced thermal shock and comparing the response of the two carbon-based structures. Primary objectives of the experiment was the confirmation of the superior thermal shock absorption of C/C structures, as compared to graphite, and the generation of precise beam shock response data to facilitate calibration of numerical models.

To assess the long-term exposure of target and collimation materials to energetic protons and the evolution of their physio-mechanical properties resulting from irradiation damage several irradiation campaigns were launched using the 200-MeV proton Linac at BN Brookhaven Linear Isotope Producer (BLIP). These irradiation damage campaigns were conducted at two different energies of the Linac (200 MeV and 181 MeV) and under different environmental conditions such as vacuum, inert gas and direct contact with the ionized target cooling water at the BLIP. The experimental matrix, in addition to the proton energy and the irradiation environment which in turn dictated the irradiation temperature, included 2D and 3D C/C structure, MoGRCF and graphite, the latter as a comparative basis.

The first irradiation campaign took place in 2004 as part of low-Z pion production target search for the Neutrino Factory-Muon Collider initiative. A total flux of protons incident onto the 3D C/C samples was $3.7 \cdot 10^{20}$ at energy of 130-140 MeV (proton energy from Linac at 200 MeV). Based on the proton beam Gaussian transverse profile characterized by $\sigma_x = \sigma_y = 7.2$ mm the peak fluence achieved during irradiation was $1.13 \cdot 10^{20}$ p/cm².

Irradiation damage of the 2D C/C structure (Toyo-Tanso AC-150) for use as a primary collimation material in Large Hadron Collider (LHC) was performed in 2005 using 200 MeV protons at BLIP. A total flux of protons incident onto the 2D C/C samples was $2.43 \cdot 10^{21}$ at energy in the interval of 195-120 MeV (depending on the sample position in the array along the beam). With a proton beam Gaussian transverse profile characterized by $\sigma_x = \sigma_y = 6.1$ mm the peak fluence achieved during irradiation was $\sim 5.2 \cdot 10^{20}$ p/cm².

The 2005 irradiation campaign was followed by the 2006 irradiation experiment which aimed to compare irradiation damage under long exposure at low temperatures (<100°C) and identical conditions of 2D C/C, 3D C/C and IG43 graphite. The irradiated array were under direct contact with the ionized cooling water (as in 2004 and 2005 campaigns) and achieved a total flux of protons of $1.1475 \cdot 10^{21}$ but with a much tighter beam spot of $\sigma_x = 4.1$ and $\sigma_y = 4.5$ (see Figure 9).

A long term exposure of 3D C/C along with several grades of graphite and h-BN were conducted at BNL in 2010 under the objectives of Long Baseline Neutrino Facility (LBNF) of the Deep Underground Neutrino Experiment (DUNE) exploring radiolytic effects on accelerating damage in carbon-based materials under energetic proton beams. To achieve this goal irradiation under inert gas atmosphere (argon) and ionized cooling water were conducted simultaneously. The total flux of protons incident on the LBNF target array was $3.247 \cdot 10^{21}$ (integrated beam current $\sim 144,310$ μ A-hours) with estimated peak fluence of $\sim 6 \cdot 10^{20}$ p/cm².

Mo-Graphite compound with embedded carbon fibers (MoGRCF) for the LHC High Luminosity upgrade was irradiated in vacuum using 200 MeV protons from the BNL Linac in 2013-14 beam runs reaching a total of $\sim 134,000 \mu\text{A}\cdot\text{hours}$ ($3.015 \cdot 10^{21}$ total proton flux and fluence of $\sim 5 \cdot 10^{20}$ p/cm²). Because of the vacuum conditions inside the special capsules containing the MoGRCF samples, the irradiation temperature was estimated to be $\sim 418^\circ\text{C}$. While not reported in this paper, a follow-up irradiation experiment of two new MoGRCF grades (lower Mo content) along with 2D C/C (Toyo Tanso AC-150) is planned for the spring of 2016 to be performed under vacuum aiming to reach a total flux of $\sim 10^{21}$. Results of this study, including post-irradiation analysis, will be presented in an upcoming paper.

In addition to proton-irradiated C/C fiber reinforced composites and fiber reinforced compounds irradiation experiments utilizing spallation neutrons (primarily fast neutrons) exploring the use of the C/C structures and graphite in fusion reactor applications have been integrated with the experimental matrix at the BNL BLIP. The objective of these studies which are only partially complete (post-irradiation analysis of 3D C/C is underway) is to compare the effects of energetic protons with those induced by fast spallation neutrons and establish damage and material property evolution correlation.

2.1 Thermal shock experiments – 24 GeV proton pulses

Figure 3 depicts the experimental set up of 3D C/C and ATJ graphite for the 24 GeV BNL AGS beam shock experiments. Shown is the array of Fabry-Perot fiber optic strain gages capturing the longitudinal responses that were connected to VELOCE signal processing system capable of resolving a 500 kHz response signals. Two C/C cylindrical targets (12 cm each) were placed in tandem along the 24 GeV beam and downstream of a 24 cm graphite target each instrumented with four gages.

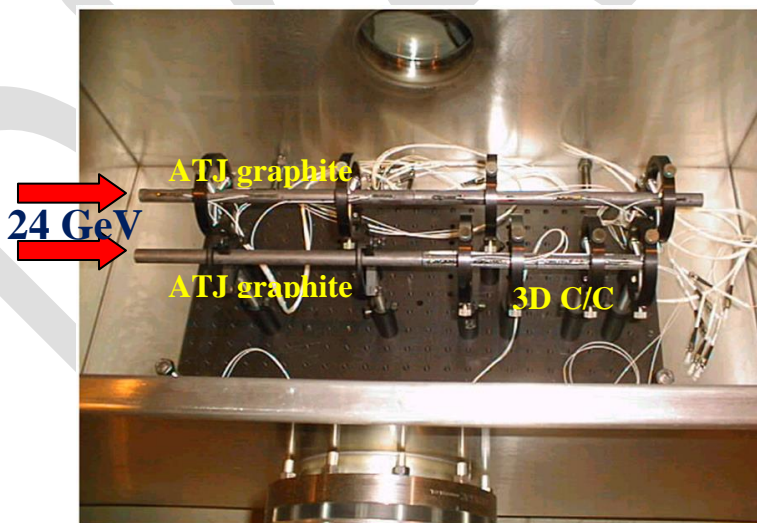


Figure 3: Set-up of instrumented 3D C/C composite and ATJ graphite targets during the E951 24-GeV BNL AGS thermal shock experiments

The experiments revealed that (a) the response of the 3D C/C is not one that would be expected by an amorphous structure (something that will be ideal for a high power target design) and (b) the intensity of the response is decreased significantly as compared to the ATJ graphite demonstrating the inherent ability of the composite to absorb thermally induced shock. Figure 4 depicts the actual micro-strain response of the different strain gages of the two 3D C/C targets indicating a global dynamic response consistent with the analytical predictions based on the density and length of the target structures. Shown in Figure 5 is the

direct comparison of captured micro-strain response between graphite and 3D C/C. It is evident from the captured response that the C/C structure significantly decreases the shock induced response as compared to graphite thus confirming the superiority of composite structures in absorbing shock. The results of the E951 experiment in addition to confirming the C/C composite structure superiority in shock absorption also provided an excellent basis for calibrating numerical models built around non-linear, transient finite element computational techniques to predict the response of graphite and composite structures to intense proton beams. Detailed comparisons of experimental (E951) data with numerical predictions are included in [Simos, et al, Ref.]

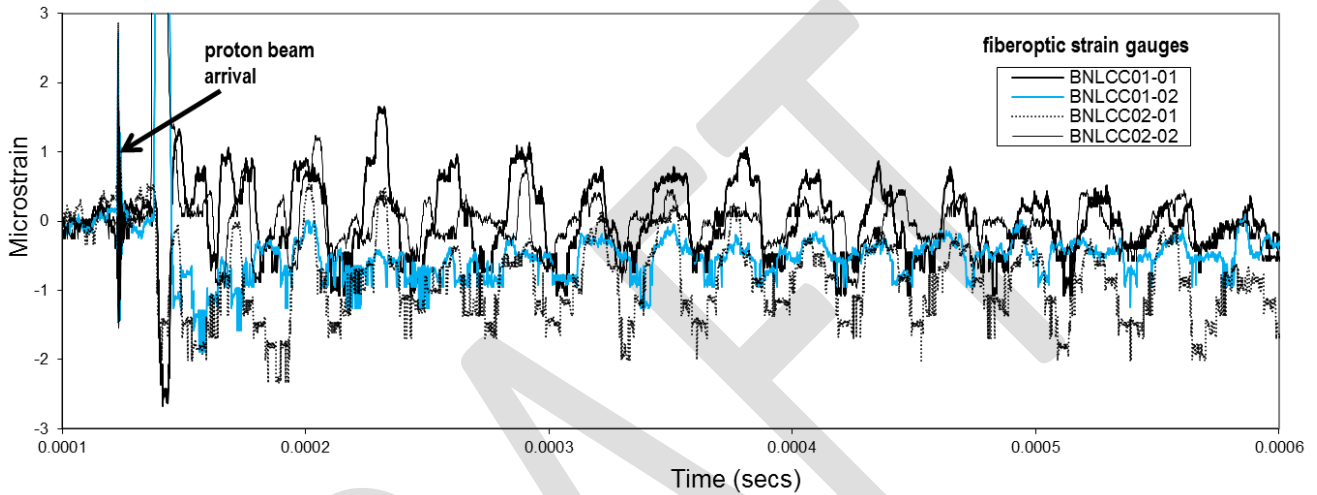


Figure 4: Fiber-optic strain gauge dynamic response resulting from 24 GeV proton pulse of intensity 3.1×10^{12} protons and beam spot of 0.7×1.7 mm RMS.

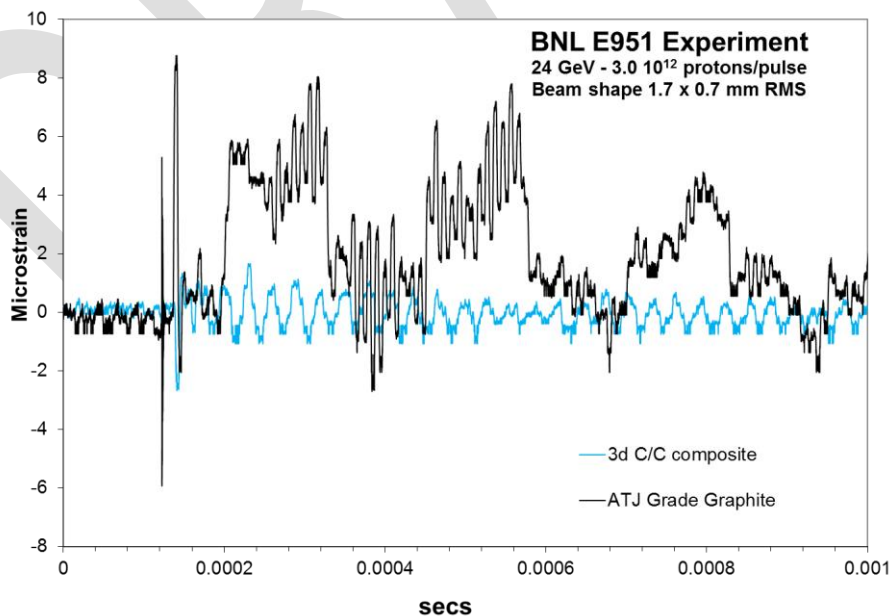


Figure 5: Direct comparison of 3D C/C response to the response of graphite subjected to the same intensity pulse

2.2 Irradiation Damage Experiments

Irradiation damage experiments were conducted at BLIP beamline of the BNL accelerator complex and in tandem operation with medical isotope production which typically utilize the 118 MeV proton energy modes from the source and Linac. To conduct irradiations either at 200 MeV or 181 MeV the energy through the Linac is increased to the desired mode, the array under proton irradiation is placed at the upstream position (of the two available) with the isotope array placed downstream and the second position. The irradiation array and the cooling between the specially designed capsules are precisely selected with the help of particle tracking codes^[21, 22, 23] such that the proton energy at the isotope target array is identical to the energy of the 118 MeV operations. Figure 6 depicts the exact geometry and set up used to simulate energy loss and desired beam profile (left) along the proton beam for the 200-MeV irradiation of MoGRCF and the actual target capsule array (right) lowered into the proton beam. Figure 7 depicts code estimated^[22, 23] proton profile through the entire array (protons/primary) satisfying both the requirement that the energy over the isotope producing array is undisturbed and that proton beam is fully arrested in the specially designed beam stop.

Shown in Figure 8 are various layouts of specially fabricated C/C samples (2D C/C and 3D C/C and MoGRCF) utilized in the different irradiation campaigns conducted at BNL BLIP beamline.

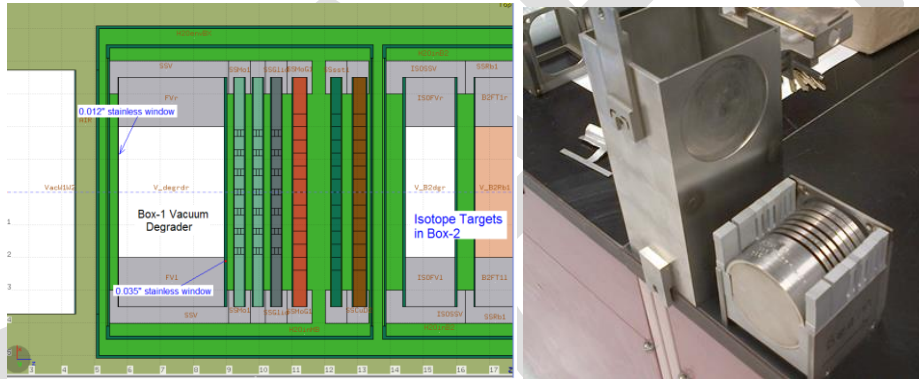


Figure 6: Proton irradiation experiment configuration and numerical modeling of proton interaction with the target array

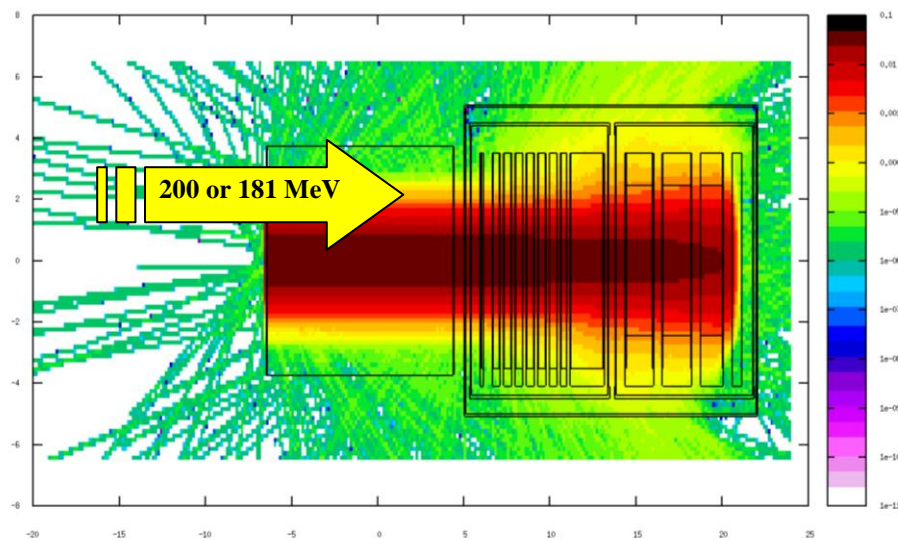


Figure 7: Numerical modeling of proton interaction with an irradiation target array in tandem with the isotope production array downstream (absica is protons/primary)

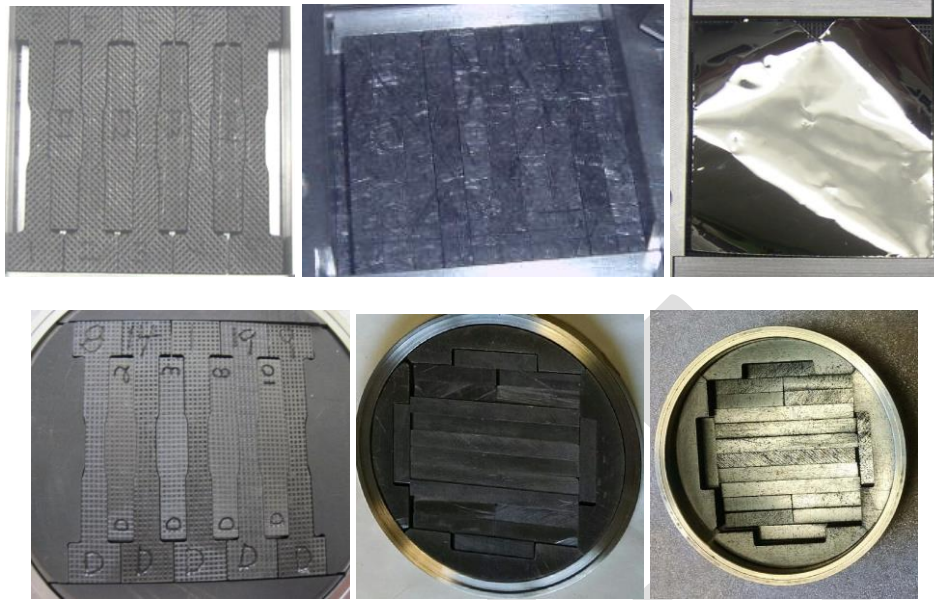


Figure 8: Layout of C/C composite specimens for proton beam irradiation. (a) 3D C/C at 45° with fiber orientation, (b) 2D C/C with fibers forming “basal” planes, (c) Ni foil placed in front of 3D C/C array for post-irradiation analysis of proton beam position and shape, (d) 3D C/C with fibers in normal orientation in argon, (e) MoGRCF in vacuum and (f) 2D C/C in vacuum

2.3 Post-irradiation evaluation summary

The post irradiation evaluation (PIE) of the various C/C composite structures and MoGRCF compounds was multi-faceted and it included, in addition to visual inspection of the structural integrity, macroscopic and microscopic evaluation of the effects on physio-mechanical properties triggered by the proton flux. Specifically, as shown in Figure 9 which depicts selected post-irradiation condition of the C/C composite and compounds, the concern of serious structural degradation at elevated proton fluence was addressed by visually inspecting the beam footprint area of the irradiated samples for signs of integrity loss. As first observed following the 2005 irradiation (Fig. 9 top-left), the region of the AC-150 (2D C/C) within the FWHM of the proton beam exhibited extensive structural degradation which was attributed to the combination of irradiating species energy (200 MeV), rate and radiolytic oxidation. The experiment was repeated in 2006 (see Fig. 9 top-right) where in addition to the 2D C/C composite, IG-43 and 3D C/C composite was irradiated under the same conditions. In post-irradiation examination was observed and concluded that in all cases where radiolytic oxidation is a factor and for fluence $\geq 5 \cdot 10^{20}$ p/cm² carbon-based structures undergo a visible structural degradation or exfoliation. The follow-up irradiation damage campaigns addressed the environmental influence on the structural degradation by irradiating, during the 2010 experiment, 3D C/C composite in argon atmosphere and in ionized cooling water leading to a deviation between the irradiation temperatures (in argon estimated around 200°C and in direct contact with water ~100°C).

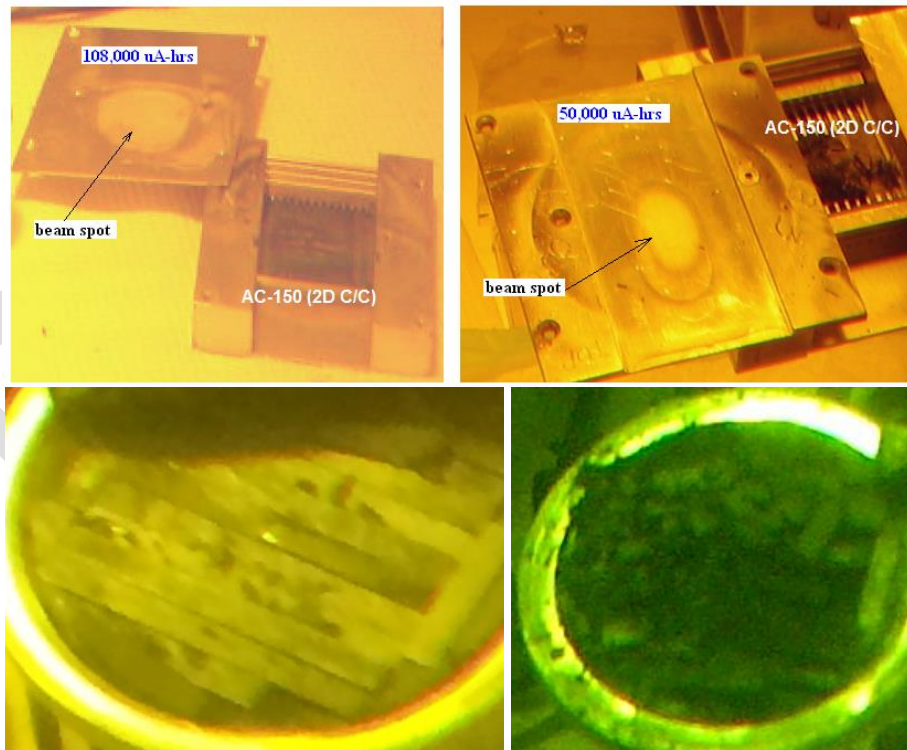


Figure 9: Observed structural degradation in irradiated 2D C/C (top) and MoGRCF (bottom). MoGRCF (bottom left) irradiated with $2.8 \cdot 10^{18}$ p/cm² at 160 MeV followed by a fast neutron fluence of $3.2 \cdot 10^{18}$ n/cm². MoGRCF (bottom right) after irradiation with $1.1 \cdot 10^{21}$ p/cm² by 160-MeV protons

The study revealed that the 3D C/C in argon and for a fluence of $6 \cdot 10^{20}$ p/cm² reached appeared to have maintained its structural integrity while its counterpart irradiated in ionized water to the same fluence showed signs of serious degradation similar the damage observed in previous studies. The effect of proton irradiation at these fluence levels on the microstructure and lattice structure of the C/C composite in argon

was studied in detail using X-ray diffraction and it will be discussed in detail in subsequent section. To further explore the influence of the irradiating environment MoGRCF compound that is dominated by graphite behavior was irradiated under vacuum for two fluence levels, one at $2.8 \cdot 10^{18}$ p/cm² at 160 MeV followed by a fast neutron fluence of $3.2 \cdot 10^{18}$ n/cm² (Figure 9 bottom-left) and one to $1.1 \cdot 10^{21}$ p/cm² by 160-MeV protons at an irradiation temperature of $\sim 428^\circ\text{C}$. It is evident from the optical images taken after irradiation that the MoGRCF which exceeded the fluence threshold associated with radiolytic oxidation has experienced serious structural degradation. Planned experiments to a lower fluence will explore the triggering fluence point.

Following assessment of the status of structural integrity following irradiation (visual inspection and structural integrity assessment a series of macroscopic and microscopic post-irradiation evaluations were conducted at the isotope processing facility hot cells and the NSLS synchrotron. These included:

- **Gamma Spectra** of irradiated MoGRCF and 3D C/C composite irradiated in ionized water and argon to assess the potential for radiochemistry taking place as a result of the environment and affecting the structural evolution. Comparative results of 3D C/C following irradiation in the two environments are shown in Figure 10.
- **Dimensional stability, CTE.** Using a horizontal, two-rod LINSEIS high resolution dilatometer (nm-level sensitivity) a comprehensive thermal analysis was performed that consisted of thermal cycling and multi-isotherm annealing.
- **Stress-strain analysis – (3PB & 4PB).** Using a 5 kN Tenius-Olsen stress-strain apparatus in combination with specially designed fixtures that facilitate Three- and Four-Point-Bending the stress-strain and load-deflection behavior of irradiated C/C and MoGRCF samples was deduced.
- **X-ray Diffraction Analysis.** Using high energy (200 keV) white x-rays at the X17B1 beamline of NSLS in conjunction with EDXRD technique and XRD technique with 70 keV monochromatic x-rays at the X17A NSLS beamline the effect of proton irradiation on the lattice structure was studied.

3. RESULTS

3.2 Post-Irradiation Evaluation

Using a high sensitivity ORTEC Ge detector the isotope signatures and photon spectra of the irradiated 3D C/C in argon and in contact with water were obtained and shown in Figure 10. As it can be observed no significant difference in the photon spectrum can be identified indicating that no radiochemistry is taking place impacting the C/C structures.

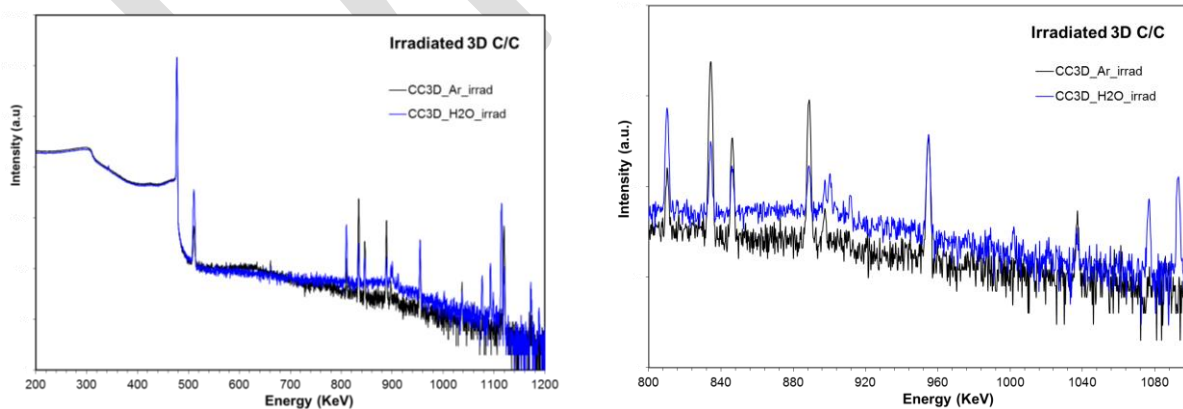


Figure 10: Photon spectra of C/C composite (3D) irradiated at $6 \cdot 10^{21}$ p.cm² in argon atmosphere and direct contact with de-ionized cooling water

3.3 Stress-strain during post-irradiation

The role of proton irradiation on C/C composites in changing the microstructure and leading to the

increase in tensile strength and Young's modulus has been studied using a 5kN tensile test system (Tenius-Olsen). Post-irradiation tests, along with tests on unirradiated samples, were performed using the specially designed three- and four-point bending fixtures. Figure 11 (left) compares the unirradiated 3D C/C structure with graphite showing both repeatability of the stress-strain test and the higher strength achieved with the fibers. Figure 11 (right) was deduced following irradiation to $1.1 \cdot 10^{20} \text{ p/cm}^2$ and depicts the change in E modulus with fluence. The tensile stress data of the irradiated 3D C/C shown are incomplete as noted in the Figure 11 caption.

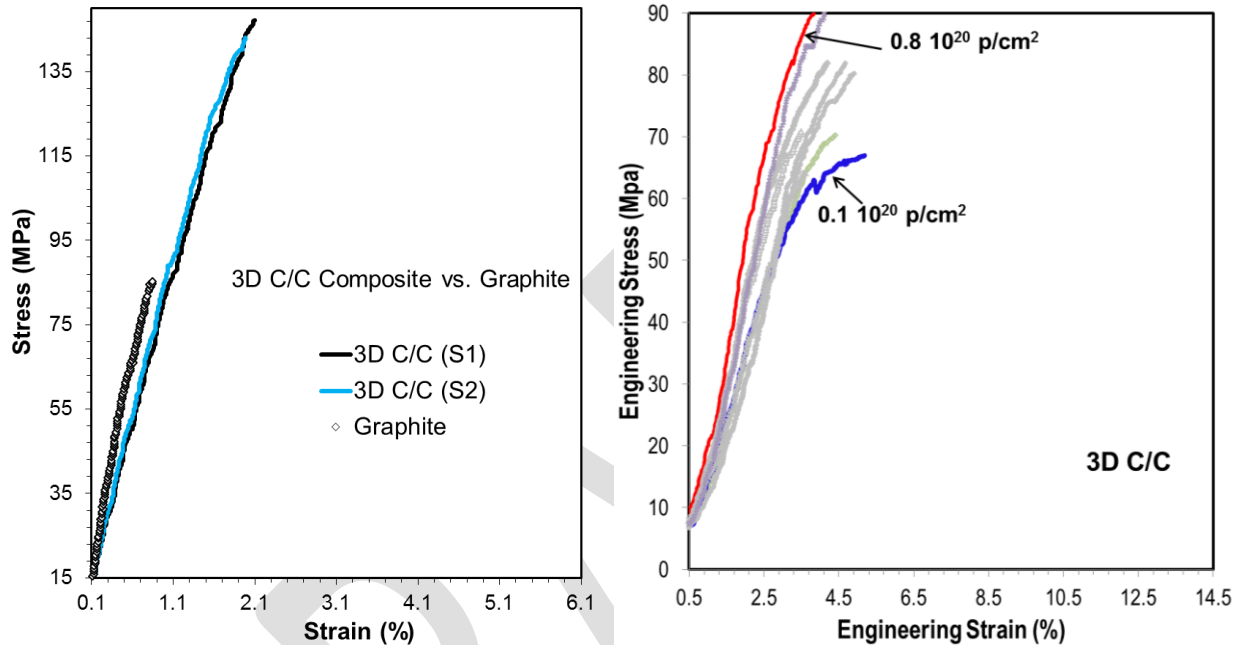


Figure 11: Tensile tests on “dog-bone” shaped 3D C/C proton-irradiated samples at $\sim 100^\circ\text{C}$ while directly cooled by ionized water. Shown at left is a direct comparison with unirradiated graphite. The effect of proton irradiation is shown at right. Premature failure at the head prevented the completion of the upper part of the stress-strain curve. The test however allowed for establishing the increase in the effective Young's modulus as a function of proton fluence.

Three point bending results of irradiated 3D C/C to a fluence of $6 \cdot 10^{21} \text{ p/cm}^2$ in terms of load-deflection relationship are shown in Figure 12 where unirradiated samples are compared with two samples (one of peak fluence (S1) and one of lower fluence (S2)) following irradiation in argon atmosphere and one at peak fluence in ionized water. What is clearly observed is that the unirradiated sample (due to relative sliding of the reinforcing fibers) experiences large deflection before failure. The increase in E modulus is observed as a result of increased fluence. The radiolytic effects on the irradiated sample in ionized water are clearly visible reducing the load capacity of the cross section significantly. Figure 13 is reproduced from Ishida et al [] and compares load-displacement curves for graphite, 1D and 2D C/C composites heat treated at different temperatures exhibiting similarities with the three-point bending load-deflection results of irradiated 3D C/C composites of Figure 12. Tension test results of irradiated 3D C/C samples produced at 45° with the horizontal (basal) fiber mesh are presented in Figure 13. With these sample orientations the strength of the matrix, rather than that of the fibers, were sought. The results indicate that the orientation is extremely weak (only a fraction of the strength in 0° orientation) and there is significant effect from irradiation.

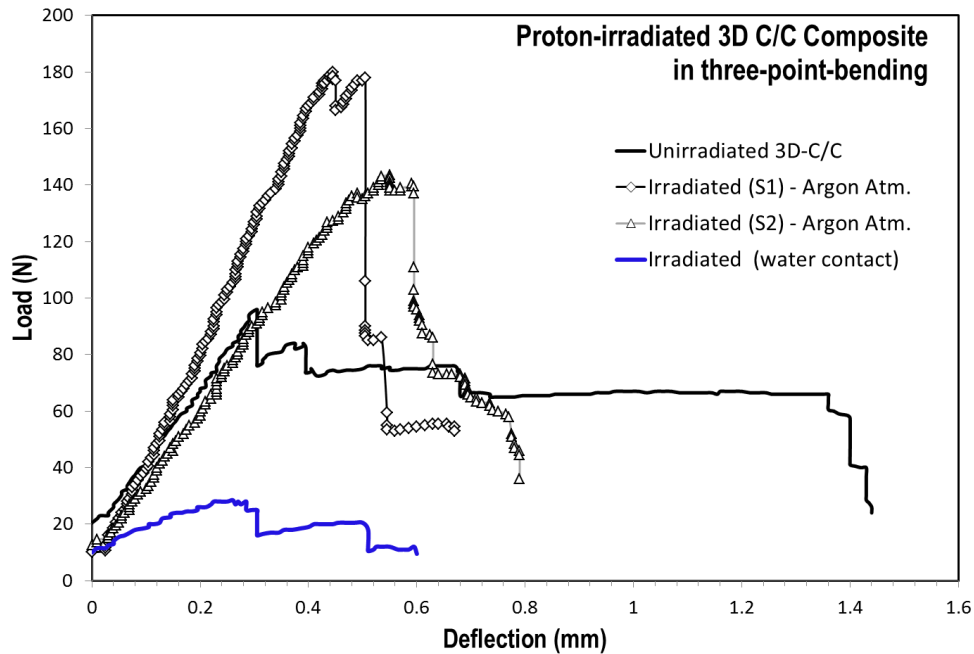


Figure 12: Three-point bending test results of 3D C/C composites irradiated in argon atmosphere and in ionized cooling water at a fluence of $\sim 6 \times 10^{20}$ p/cm²

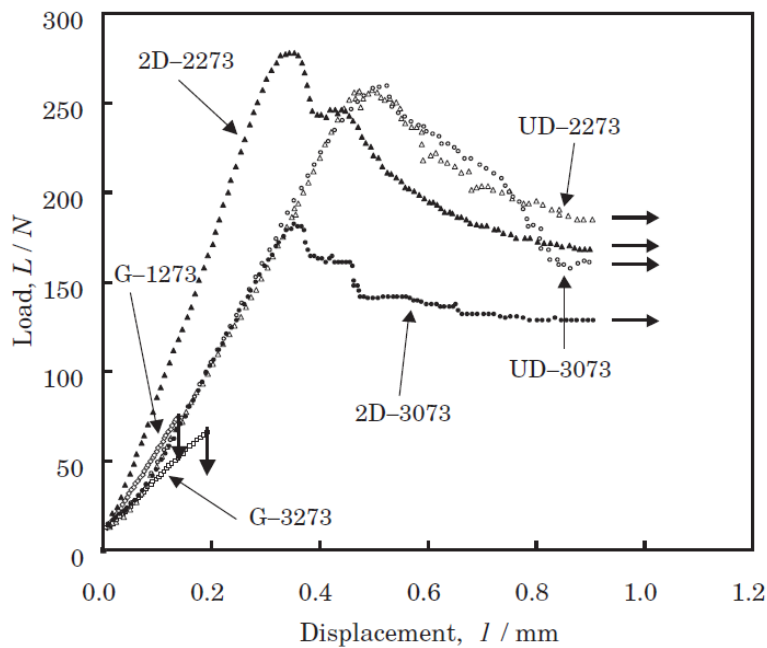


Figure 13 (after Ishida et al): Load and displacement for C/C composites and graphites. G-1273 and G-3273 indicate graphites heat-treated at 1273K and 3273 K, respectively. UD-2273 and UD-3073 represent C/C composites heat-treated at 2273K and 3073 K, respectively, whose fiber orientations are unidirectional. 2D-2273 and 2D-3073 indicate C/C composites heat-treated at 2273K and 3073 K, respectively, with 2-D fiber orientations.

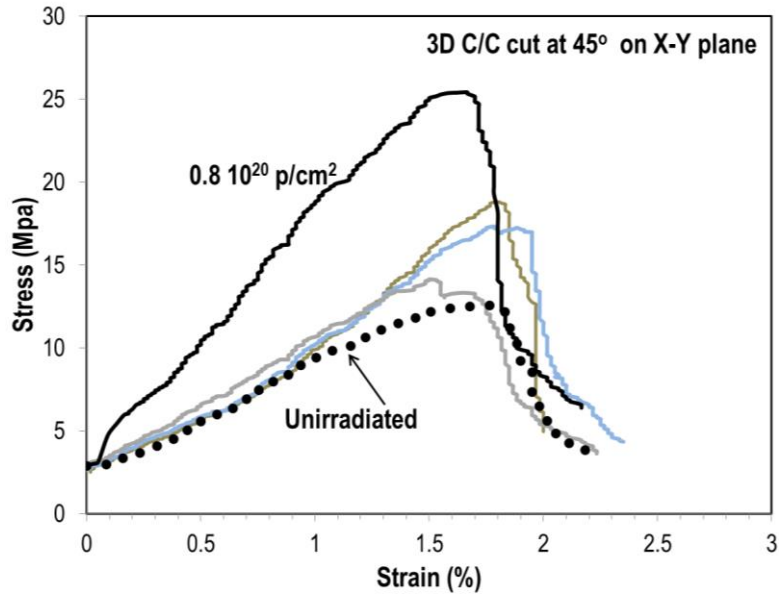


Figure 13: Tension test of 3D C/C composite samples cut at 45-degree with fiber “mesh” in the horizontal planes

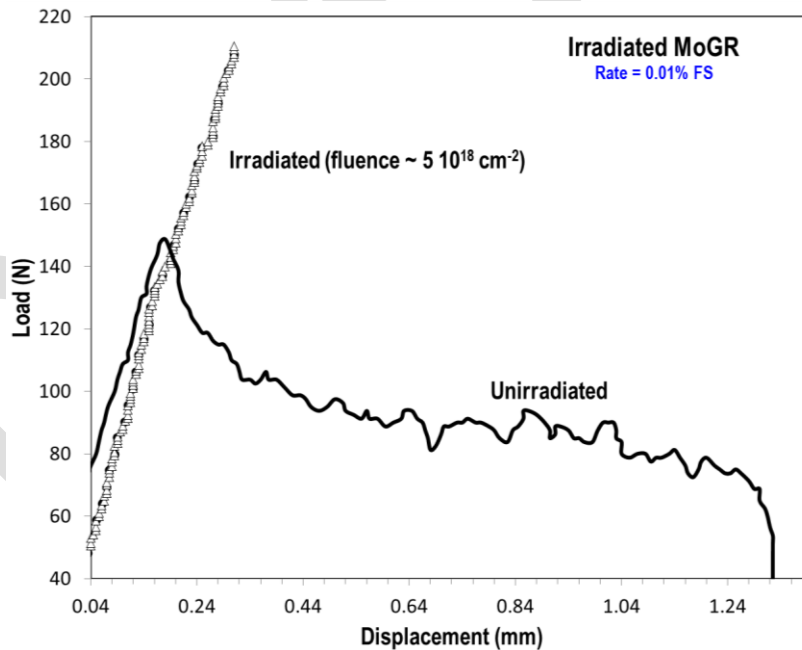


Figure 14: Four-point-bending test comparison of irradiated and unirradiated MoGRCF. Shown is the characteristic kinking appearing to shift upwards with irradiation. Also clearly depicted is the increase in the effective Young’s modulus (change of slope).

Figure 14 compares load-deflection results of unirradiated and irradiated MoGRCF compound. While the unirradiated MoGRCF response resembles that of C/C composite, a significant change occurs following irradiation. The absence of a “continuous” net of carbon fibers in the compound leads to the cross section of the bar type specimen (4mm x 4mm) to exhibit no “yield”.

To further understand the structure of the compound, ultrasonic velocities were deduced from a longitudinal transducer using the pulse echo technique and direct contact with the sample with the help of a coupler layer. The ultrasonic tests had as objective the qualitative evolution of the microstructure resulting from irradiation. The study revealed that a significant anisotropy exists in the structure of the formed alloy prior to irradiation. Measurements of ultrasonic velocities showed that the velocity is of the order of 1,530 m/s in the “weak” direction and 2,956.5 m/s in the “denser” direction. Relatively low dose irradiation by 160 MeV protons (order $\sim 10^{18}$ protons/cm²) over a section of the specimen followed by almost uniform mixed spectrum irradiation dominated by fast neutrons revealed that observable increase in the ultrasonic velocity resulted from such irradiation dose. Along the “weak” direction ultrasonic velocities approach 2,000 m/s or an increase of $\sim 30\%$ and along the “stiff” direction approach 3,600 m/s or an increase of $\sim 21\%$.

3.4 Thermal Stability and CTE

Dimensional stability as a result of proton irradiation that is accompanied with temperature increase and during temperature excursions either in the target or the collimation element is of paramount importance and design consideration. Carbon fiber reinforced structures are more prone to experience dimensional change because the unique structure (fiber mesh integrated with graphitized matrix) and the high degree of anisotropy. Figure 15 depicts the CTE of unirradiated 2D C/C structure as a function of temperature. Observed is the significant variation with temperature and the anisotropy that exists. A low value, negative coefficient exists along the fibers while normal to the planes where the structure resembles stacking of graphite basal planes the CTE is increasing positive. The volumetric change of the 2D C/C structure with thermal cycling was studied with the results shown in Figure 16. It is observed that the structure stabilizes following thermal annealing in both longitudinal and normal to the planes orientation owed to the reduction of manufacturer porosity and thermally-induced growth into the pre-existing pores.

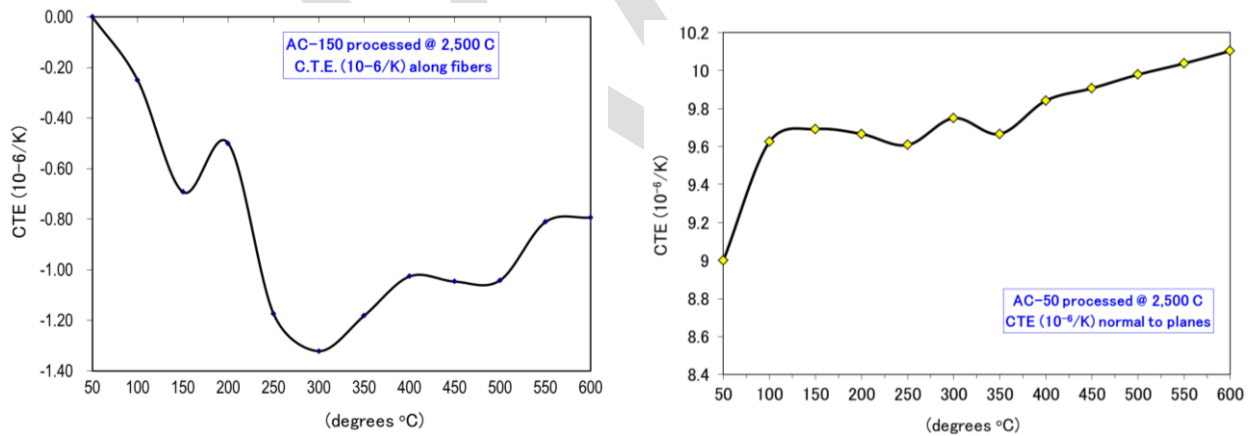


Figure 15: Thermal expansion coefficient of unirradiated 2D C/C structure (Toyo-Tanso AC-150) along the two fiber orientations as a function of temperature.

The results of post-irradiation annealing of the AC-150 (2D C/C) irradiated with 200 MeV protons to 4.5×10^{20} p/cm² is shown in Figure 17. What is observed during post-irradiation annealing is that normal to the fiber planes (Fig. 17 left) the structure contracts during the first thermal cycle at temperatures above the irradiation temperature due to annealing of interstitials in the lattice of the graphitized matrix (filler). The opposite effect is experienced along the fiber planes where the structure expands as a result of defect annealing. Important to note that during post-irradiation annealing, a fraction of the irradiation-induced dimensional change is recovered. The annealing temperature above the irradiation temperature represents

activation energy for interstitial atoms at a certain distance from the basal plane to return to empty sites in the octahedral planes causing dimensional increase along the plane. Annealing at higher temperature (as seen in Figure 17b) no dimensional change is observed up to the previously achieved temperature due to the fact that all interstitials that could be activated and return to sites on the basal plane have done so. Thus, volumetric change begins again in excess of the previous post-irradiation annealing temperature.

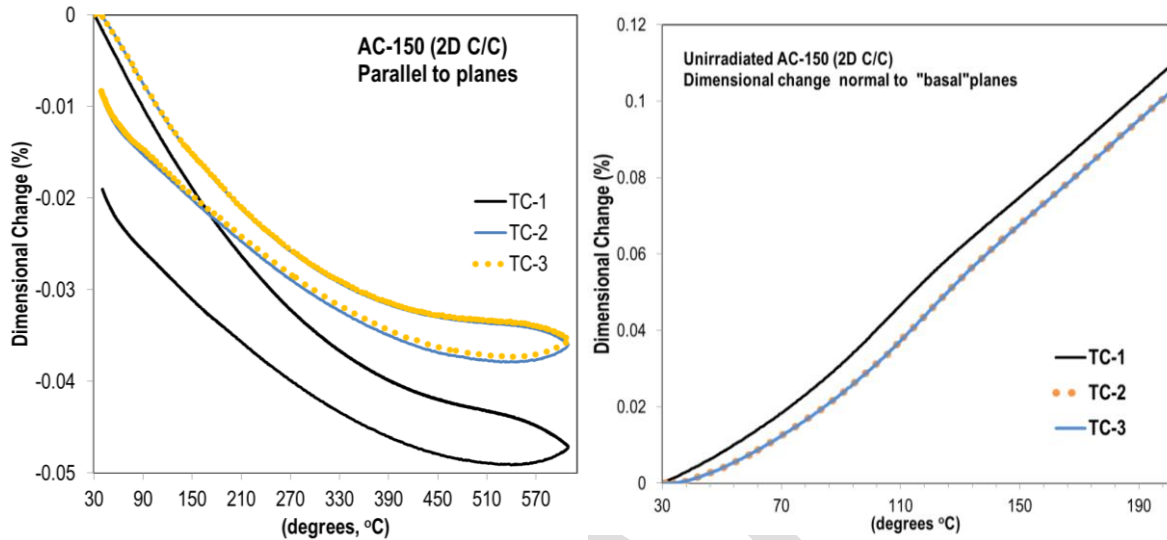


Figure 16: Pre-irradiation thermal cycle annealing of the 2D C/C structure (Toyo-Tanso AC-150) along the two fiber orientations.

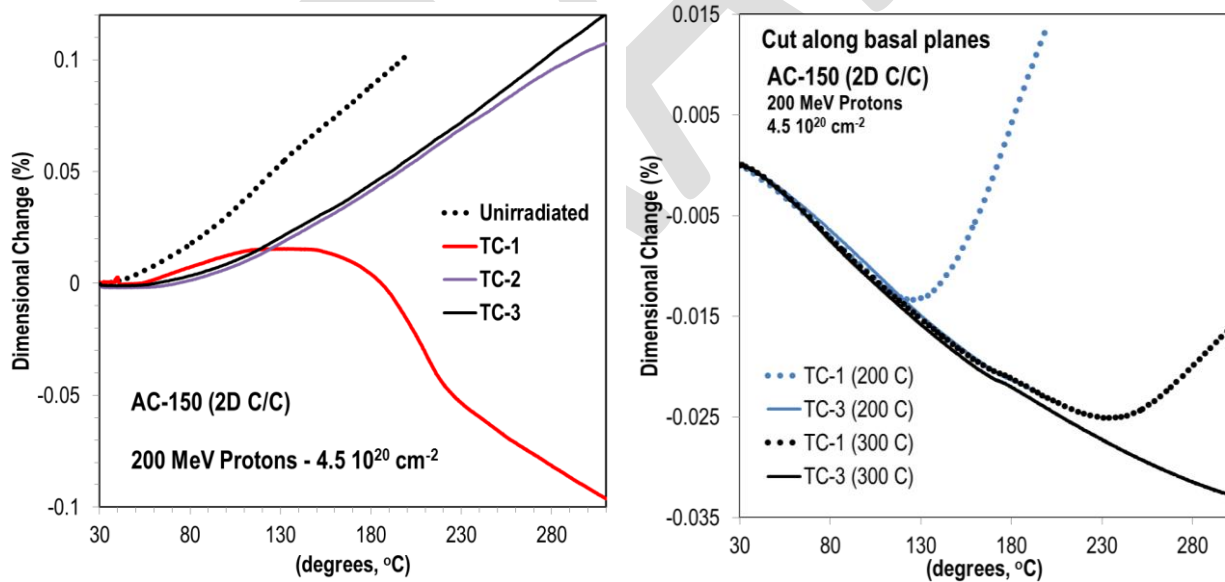


Figure 17: Post-irradiation thermal cycle annealing of the 2D C/C structure (Toyo-Tanso AC-150) along the two fiber orientations. Normal to the fiber planes (left) and along the fibers (right)

The pre- and post- irradiation annealing of 3D C/C has been studied following the irradiations with 200 MeV and 181 MeV protons. Shown in Figure 18 is the “adjustment” of the structure resulting from manufacturing porosity and defects. The evolution of thermal expansion coefficient with post-irradiation annealing and its dependence on average proton fluence received by the test sample is shown in Figure 19.

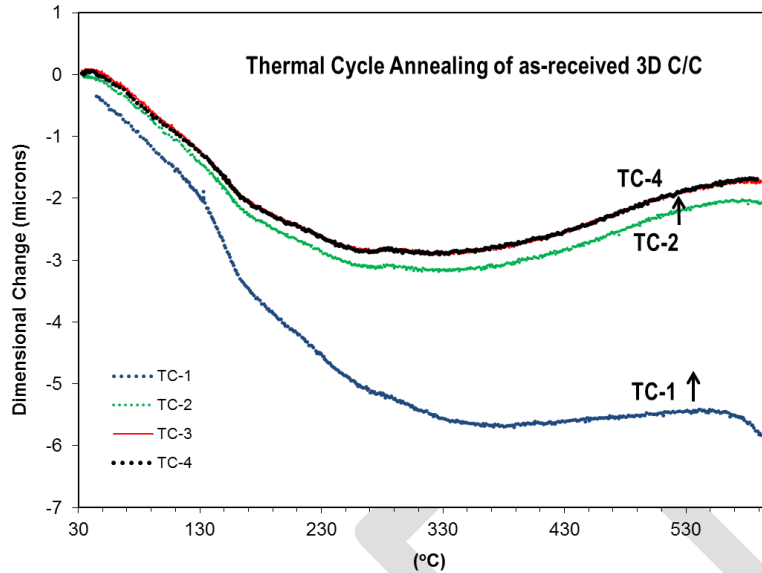


Figure 18: Pre-irradiation thermal cycle annealing of the 3D C/C structure showing achieved dimensional stability after the third thermal cycle

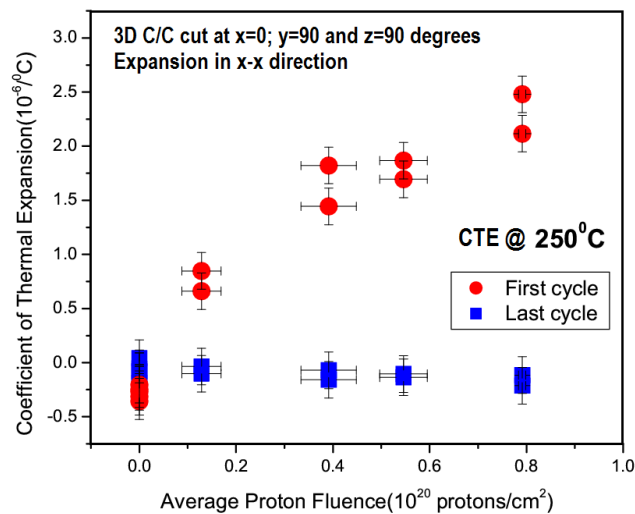


Figure 19: Thermal expansion coefficient of proton irradiated 3D C/C composite as a function of average fluence of the test specimen

The effects of higher dose ($6 \times 10^{20} \text{ p/cm}^2$) on the dimensional stability of the 3D C/C structure in combination with the irradiating environment (argon atmosphere vs. water) are shown in Figures 20-22. The annealing response is similar to the post-irradiation response exhibited by the 2D C/C structure along the fibers, i.e. above the irradiation temperature the fiber-filler matrix undergoes expansion due to the mobilization of interstitials and their return on empty sites in the lattice and on the octahedral planes. The effect of the environment post the first thermal is minimal. During the first post-irradiation cycle annealing in the material irradiated in contact with water begins earlier due to the fact that the irradiation temperature was lower, The inflection point of the curve reveals the irradiation temperature for the two environments. The effect of higher activation energies (i.e. higher annealing temperatures) on the progressive dimensional change of highly irradiated 3D C/C composite in argon is shown in Figure 22 and resembling the annealing behavior of the 2-D C/C along the fiber planes. Dimensional changes in irradiated MoGRCF compound including post-irradiation annealing are shown in Figures 23-25.

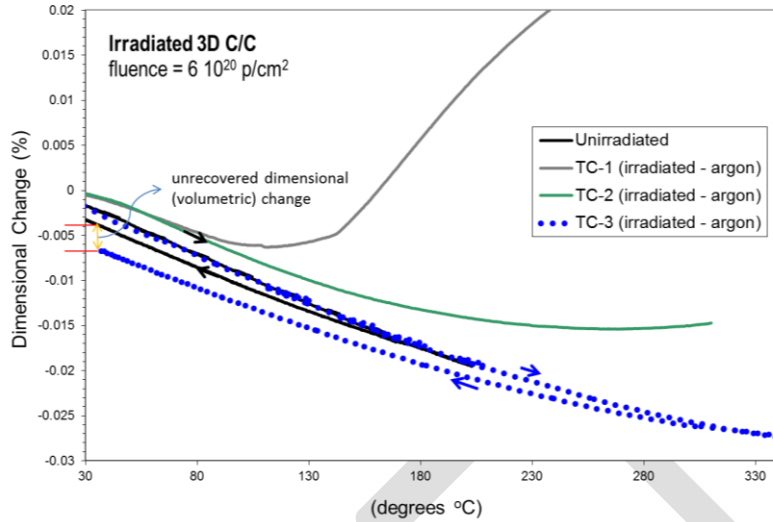


Figure 20: Post-irradiation thermal annealing of irradiated 3D C/C to high dose in argon atmosphere

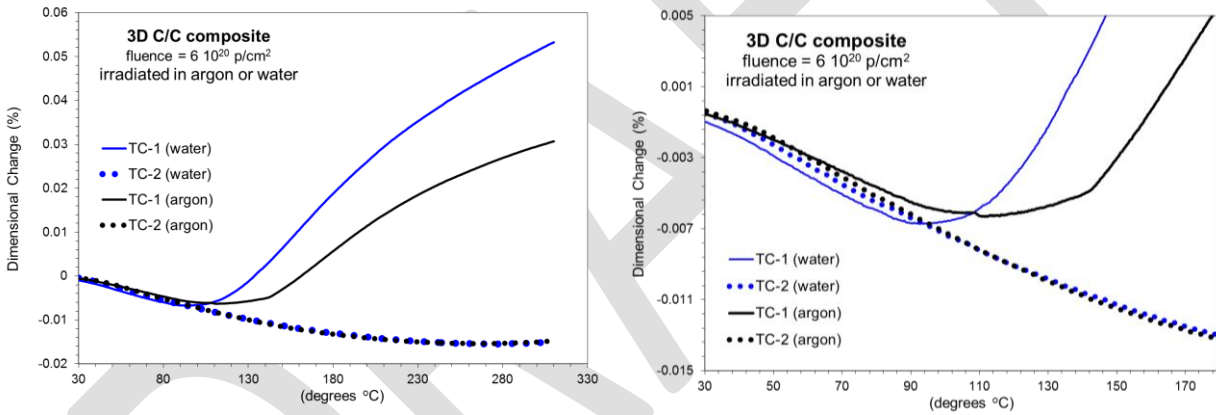


Figure 21: Post-irradiation thermal cycle annealing of proton irradiated 3D C/C to high dose comparing the effects of the irradiating environment.

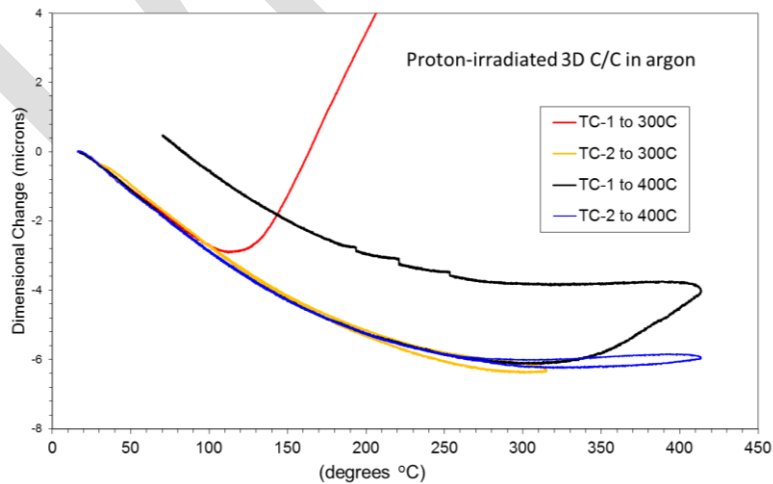


Figure 22: Post-irradiation thermal cycle annealing of proton irradiated 3D C/C to high dose comparing the effects of the irradiating environment.

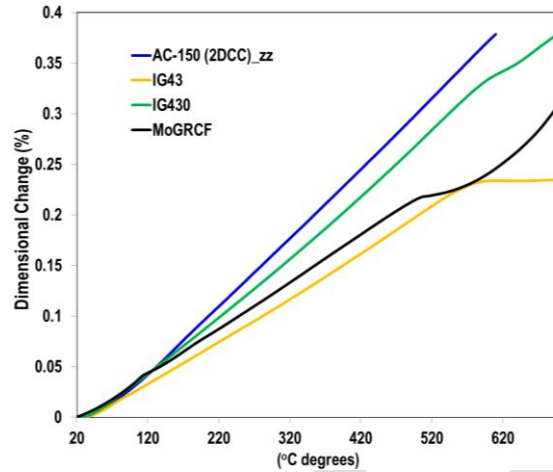


Figure 23: Comparison of dimensional change in unirradiated MoGRCF with IG-43, IG-430 and 2D C/C

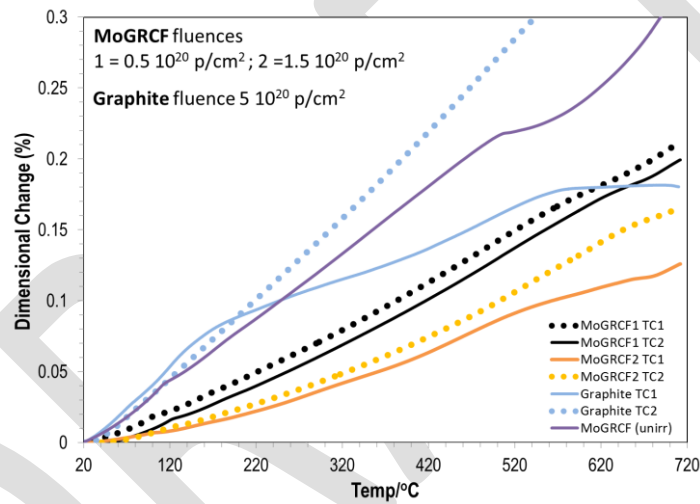


Figure 24: Post-irradiation annealing of MoGRCF compared to graphite

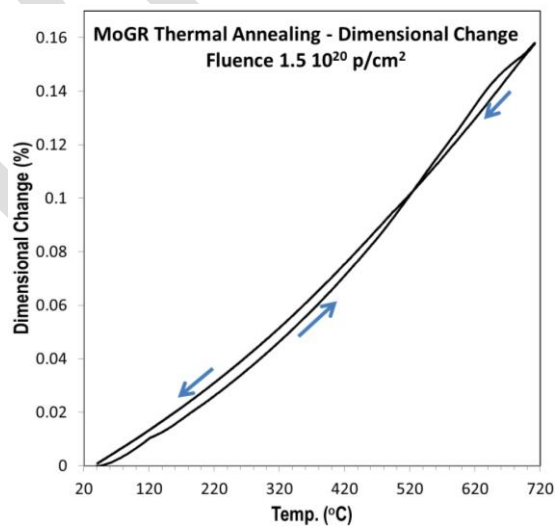


Figure 25: Dimensional change experienced by irradiated MoGRCF during a complete thermal cycle. Noted is the cross-over during the cooling phase of the cycle.

3.5 X-ray Diffraction (EDXRD) studies of proton-irradiated C/C composites

Presented in this section is x-ray diffraction results of proton irradiated C/C composite structures and MoGRCF compounds obtained using the EDXRD technique with high energy (200 keV) white beam x-rays at the X17B1 beamline of NSLS and XRD results using 70 keV monochromatic x-rays at X17A. A special experimental stage facilitating in-situ four-point-bending state of stress with x-ray diffraction of the irradiated samples has been utilized.

Depicted in Figure 26 is a 3D phase map of proton irradiated 2D C/C showing the (002) and (004) diffractions. Important to note is the “wave-like” variation on the two diffractions corresponding to the basal plane distances. One should recall that the AC-150 or 2D C/C composite consists of stacked layers of weaved fibers along the plane separated by a graphitized matrix. As noted in other studies [Paulmier et al,] lower graphitization is expected in the fibers than the graphitized matrix which in turn indicates that the inter-plane distance is larger in the fibers than in the matrix. Looking closer into the variation of the d_{002} across the thickness of the sample while scanning normal to the fiber planes we observe the variation in d-spacing depicted in Figure 27 for post irradiation analysis with no external load and under four-point-bending state of stress. One can observe the fluctuation in d_{002} resulting from alternating matrix fill and fiber planes.

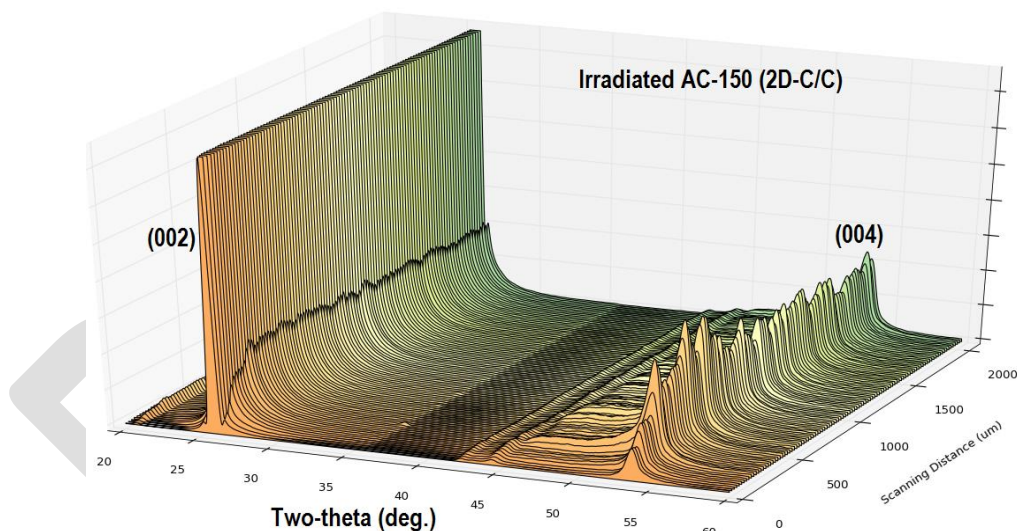


Figure 26: 3D phase map of irradiated AC-150 (2D C/C). Noted is the wave-like variation in intensity resulting from scanning over either fiber layers or the matrix

The as received and irradiated 3D C/C composite structure were characterized using the EDXRD technique. Figure 28 shows the 3D phase map of the as-received and proton-irradiated sample (fluence 6×10^{20} p/cm²). To understand the as-received structure and the processing that was used the d-spacing across the 4mm sample thickness was deduced. Shown in Figure 29 (left) is the d-spacing variation across the sample thickness and exhibiting a characteristic dip which indicates higher degree of graphitization. Shown on Figure 29 (right) is the (002) diffraction peak for the three noted locations revealing different levels of graphitization. Based on the observed large width of the (002) diffraction peak it can be deduced that the graphitization of the 3D C/C composite is low. The shoulder shown is the result of two (002) diffraction peaks, one with lower diffraction angle owed to the least crystallized phase (fiber) and the matrix.

The effects of proton irradiation on the 3D C/C composite (fluence of 6×10^{20} p/cm²) and in particular around the (002) diffraction peak are shown in Figure 30. What is observed is that the shoulder depicted

in the as-received material (indicative of less crystallized phase) has disappeared, indicating irradiation-induced crystallization) with a simultaneous appearance of a shoulder at higher diffraction angles indicating that with increasing fluence, the interstitial clusters coalesce forming new crystalline planes. Shown in Figures 31-32 are direct comparison of (002) and (112) diffraction peak evolution and c-parameter change with irradiation of graphite and 3D C/C composite following irradiation at same fluence. A comparison of the XRD spectra and d-spacing between 2D C/C and 3D C/C is provided in Figures 33 (a; b; c).

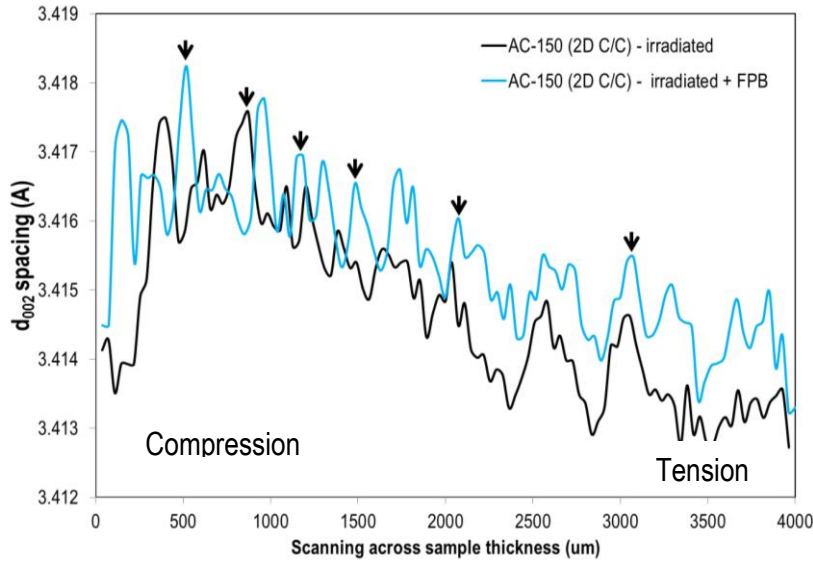


Figure 27: d-spacing variation including four-point bending (FPB) on irradiated 2D C/C with planes of carbon fibers parallel to the x-ray beam

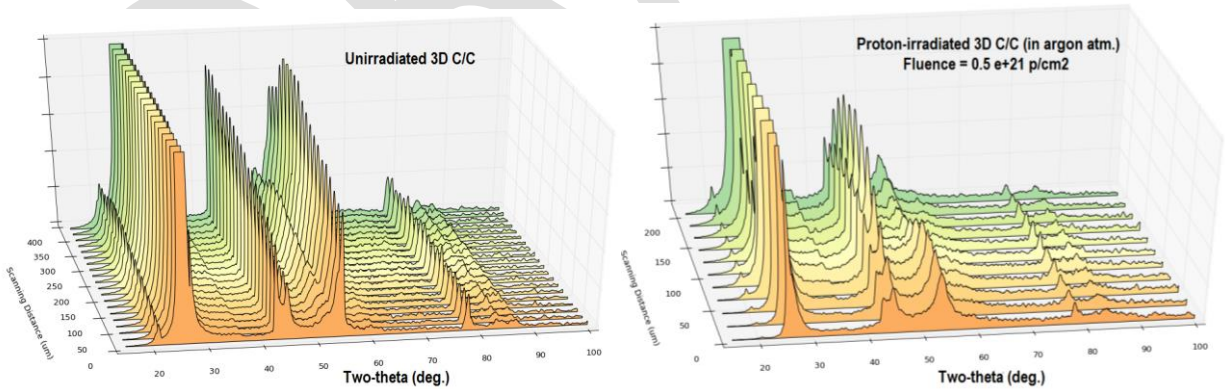


Figure 28: 3-D EDXRD phase map of as-received (left) and irradiated 3D C/C composite (right)

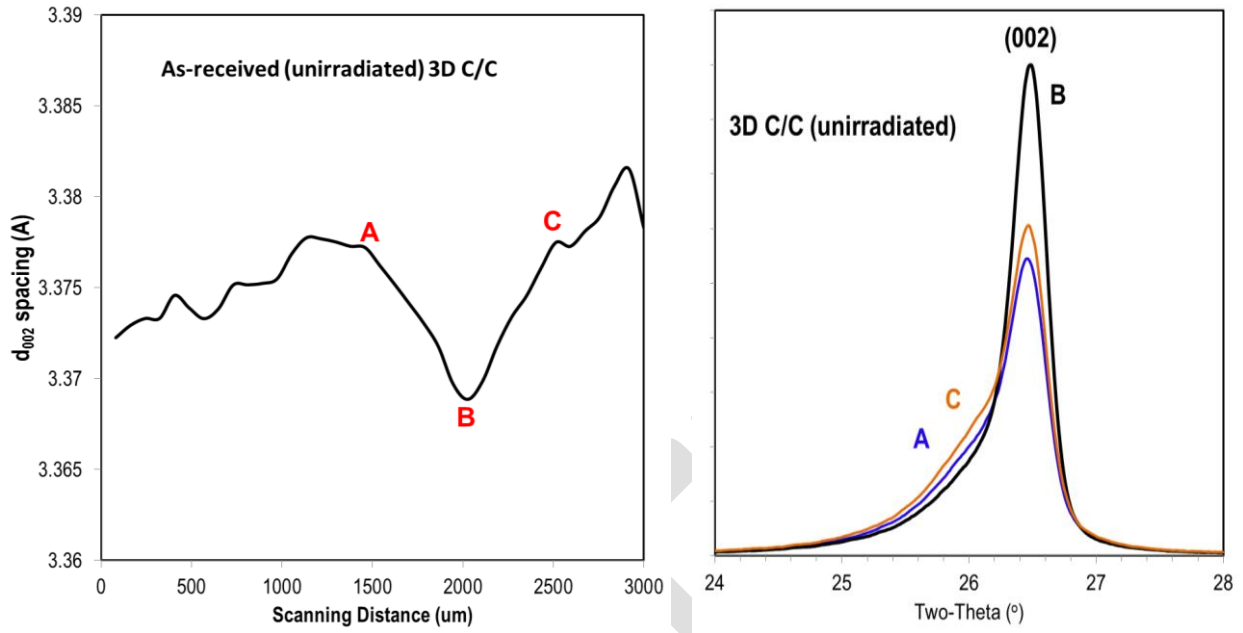


Figure 29: d-spacing and XRD spectrum of as-received 3D C/C

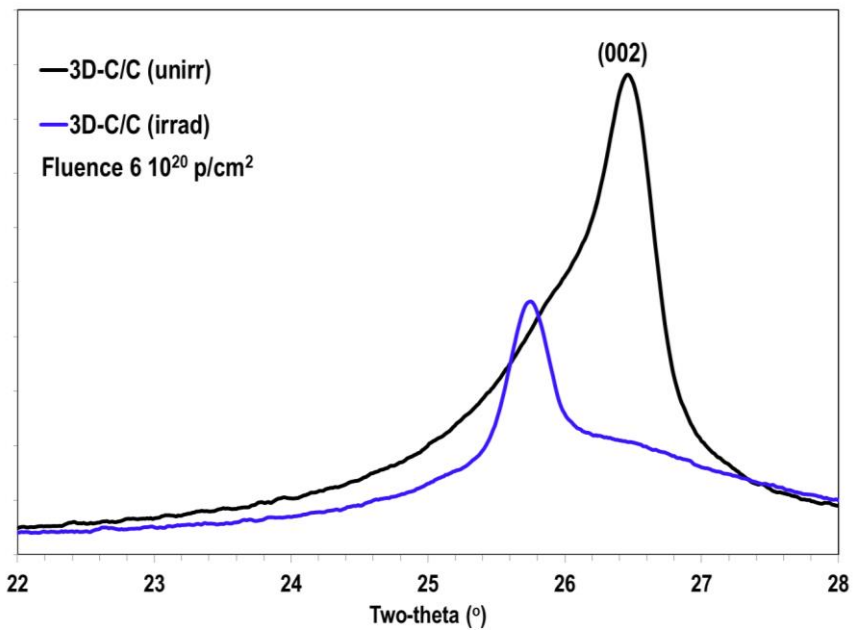


Figure 30: Irradiation-induced inter-planar change and graphitization of fibers in 3D C/C composite

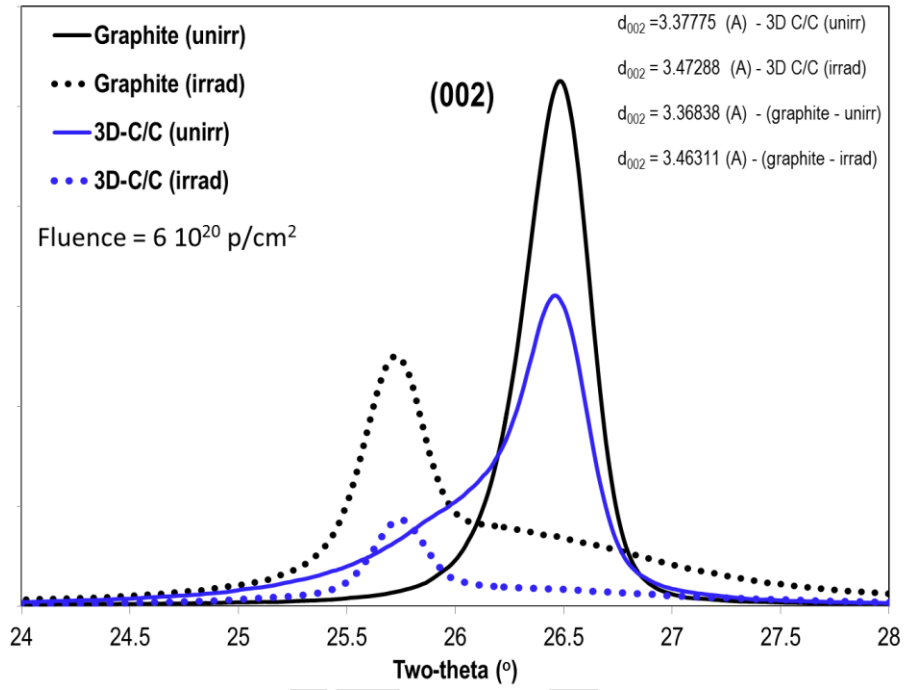


Figure 31: Irradiation-induced inter-planar change in irradiated 3D C/C compared to irradiated graphite with similar proton fluence

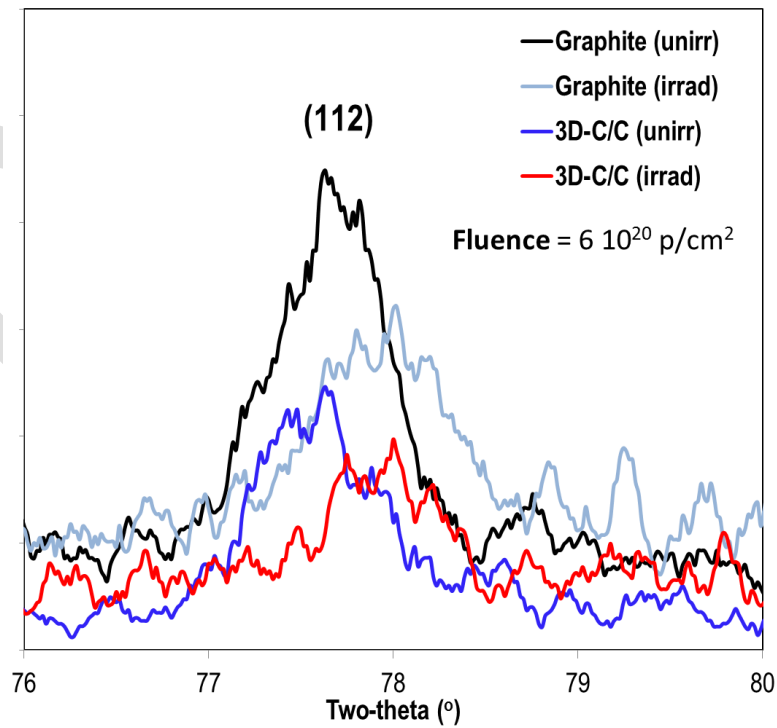


Figure 32: Irradiation-induced a-parameter change as seen by the (112) diffraction peak in irradiated 3D C/C compared to irradiated graphite with similar proton fluence

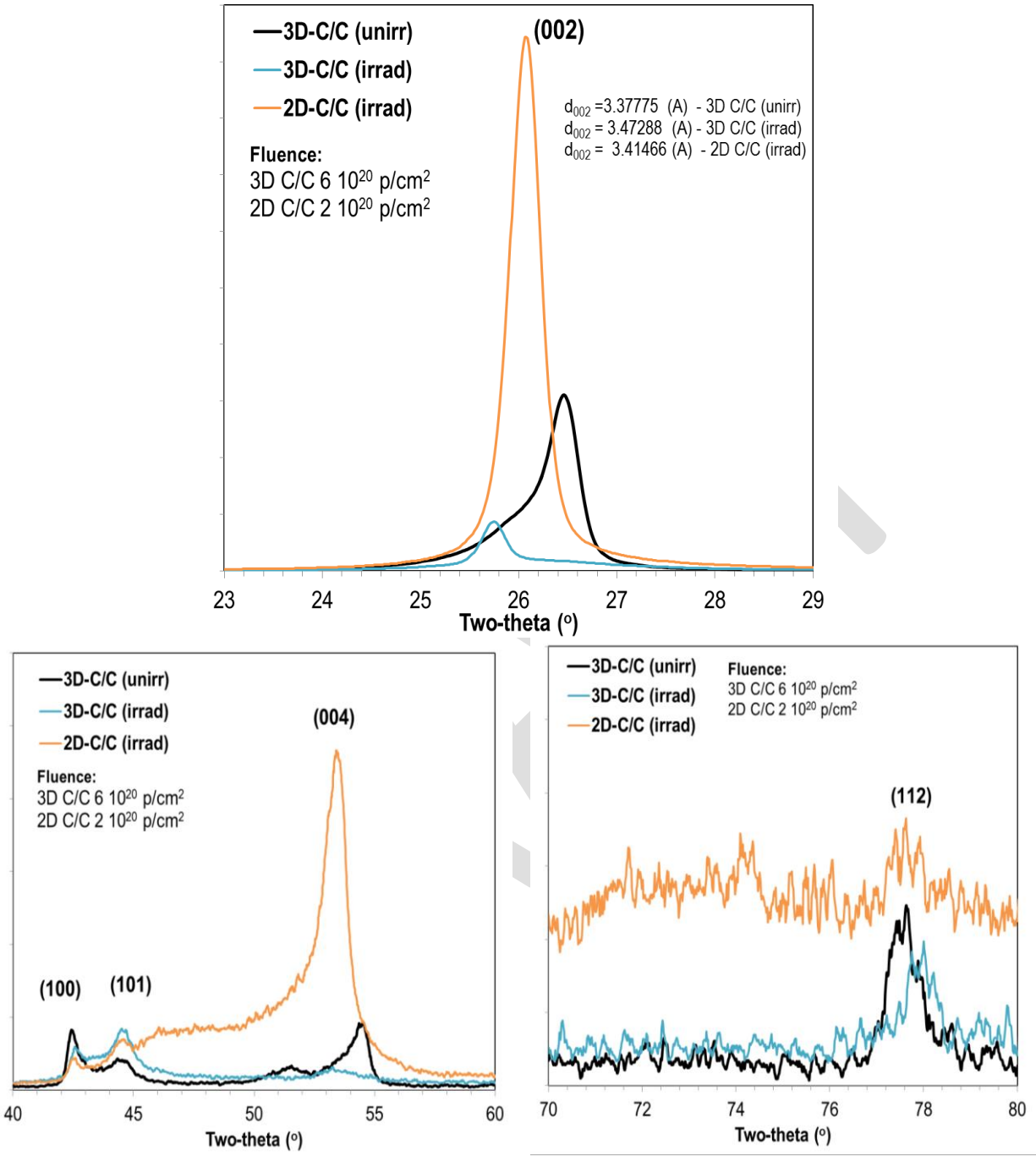


Figure 33: Irradiation-induced changes in the XRD spectra and d-spacing of irradiated 3D C/C and 2D C/C composites irradiated to different proton fluences

Monochromatic 70 keV and 200 keV white x-rays were used to assess the microstructural evolution of the MoGRCF compound with irradiation. Figure 34 depicts diffraction patterns of irradiated MoGRCF and graphite from the 70 keV monochromatic x-ray experiments performed to identify differences and similarities in the two microstructures. As shown, high degree of texture exists in the MoGRCF owed to the presence of Mo and Mo_xC_y . The 3D phase map of as-received MoGRCF is shown in Figure 35 with the (002) and (004) diffraction peaks identified in the map.

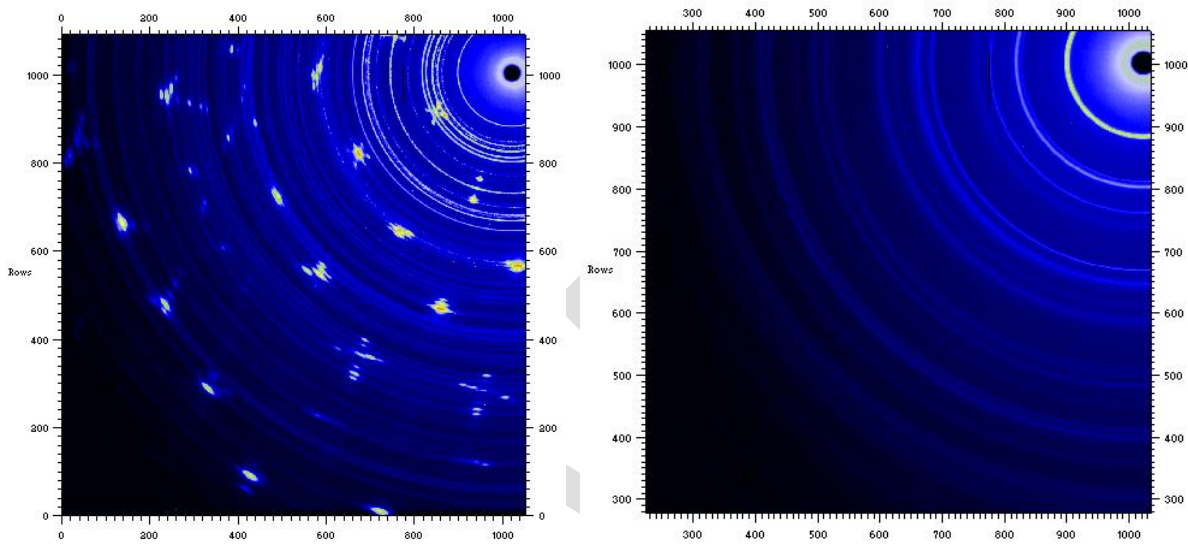


Figure 34: Diffraction pattern of irradiated MoGRCF (left) and irradiated graphite (right)

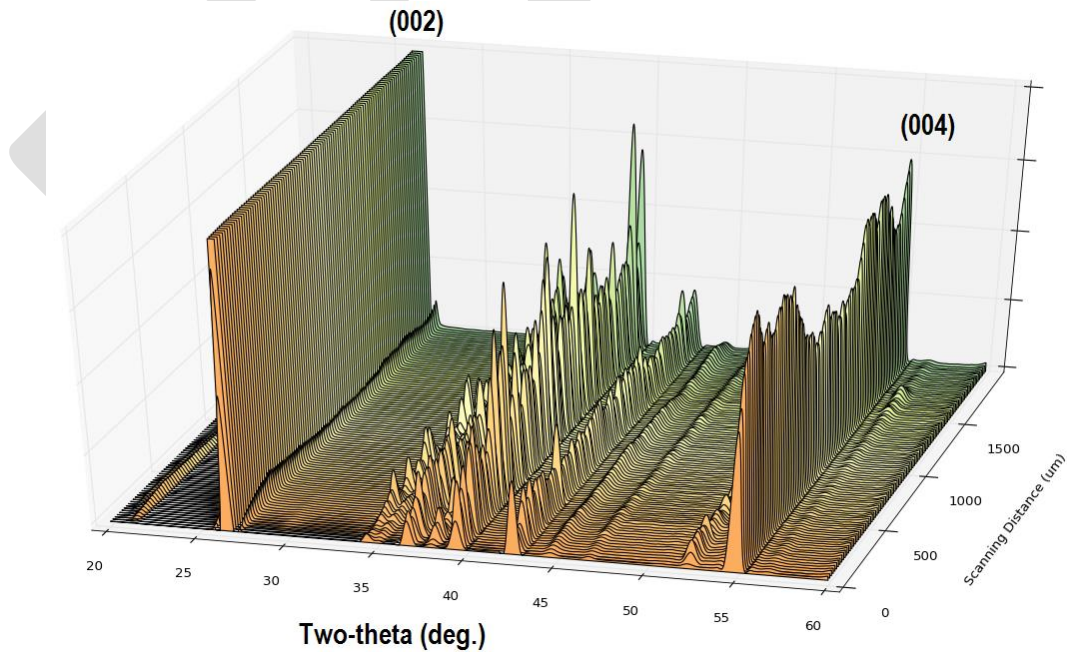


Figure 35: 3D phase map of as-received MoGRCF

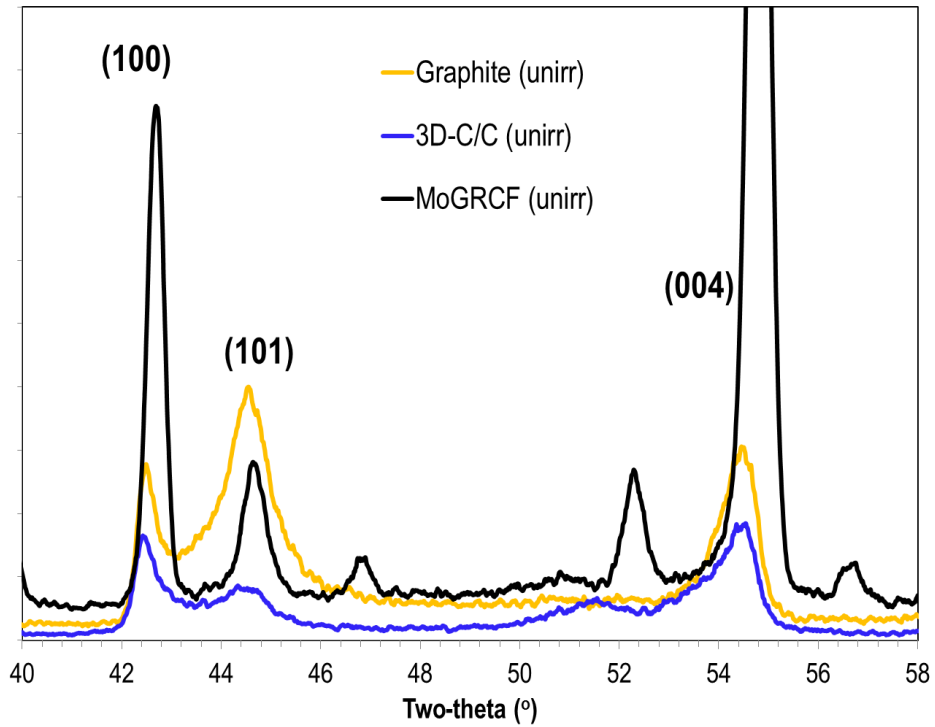
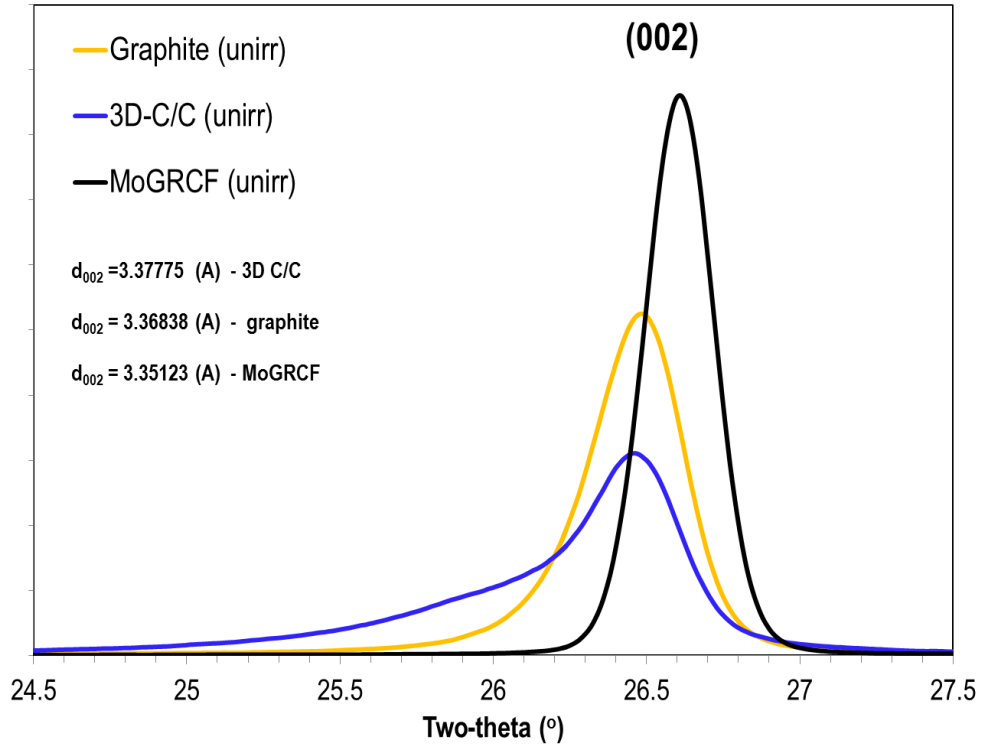


Figure 36: Comparison of XRD spectra and d-spacing between MoGRCF, 3D C/C and graphite indicating that MoGRCF has high degree of graphitization

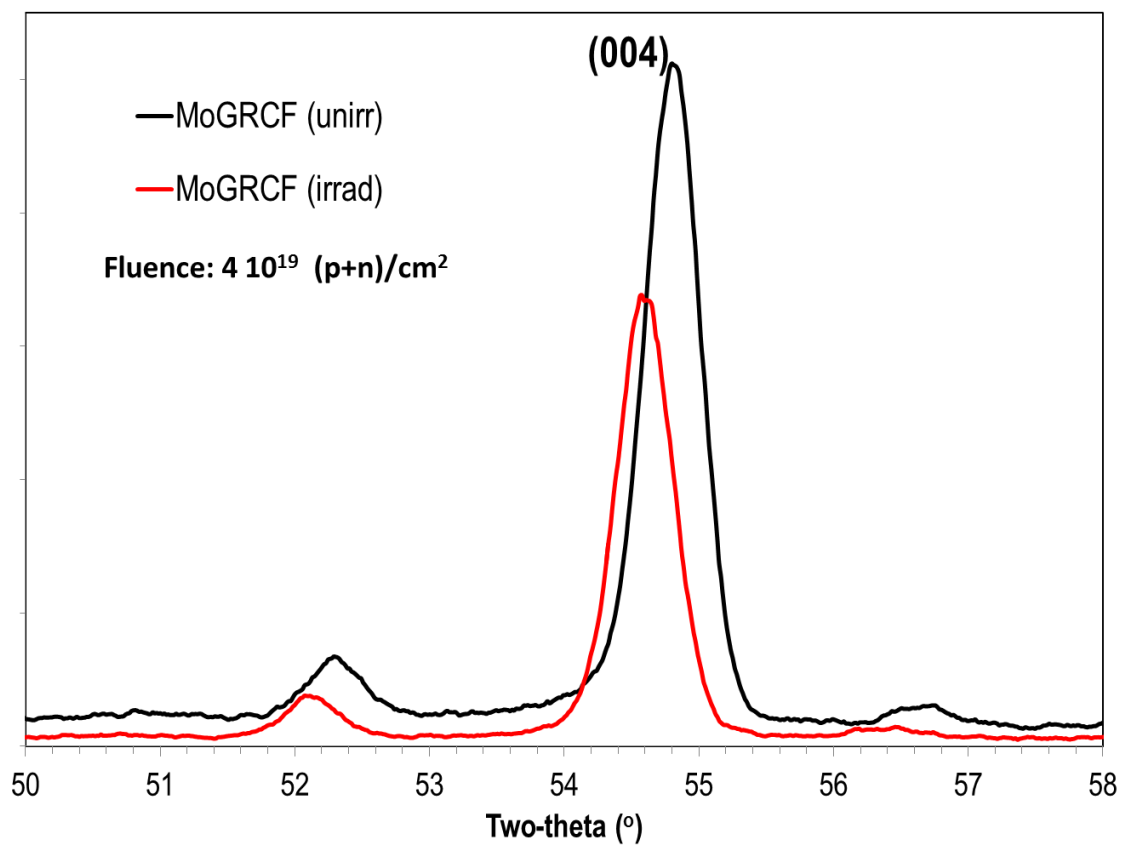


Figure 37: Irradiation-induced changes in the (004) diffraction plane of MoGRCF

4. Summary and Discussion

A multi-faceted study consisting high energy beam shock studies and a series of irradiation damage experiments at energies between 120-200 MeV, followed by macroscopic and microscopic post-irradiation evaluation, was conducted to assess the survivability and/or evolution of carbon fiber composite structures and compounds exposed to high proton fluence under various atmospheres. Macroscopic post-irradiation analysis of thermal stability, CTE evaluation, mechanical behavior and annealing for E modulus restoration were conducted at the BNL Hot Cell Facility. Microscopic post-irradiation evaluation using X-ray diffraction techniques were conducted at the BNL NSLS synchrotron using high energy polychromatic and monochromatic x-ray beams. Off-beam studies assessing C/C and Mo-GRCF metal matrix compound microstructural response to high temperature were also undertaken.

The study has revealed the following:

- 24 GeV shock experiments confirmed the superior, compared to that of graphite, ability of the 3D C/C fiber reinforced structures to absorb beam-induced shock while the experiment provided an excellent basis for calibration of numerical models utilized in high power target evaluation
- As received 2D and 3D C/C composites exhibit manufacturing defects and porosity attributed to the graphitization process and the dissimilar expansion properties between the matrix and the fibers. Thermal cycle annealing has shown to remove most of the manufacturing defects leading to a stable structure. Higher degree of dimensional stability is exhibited by 3D C/C structures.
- Proton irradiation induces swelling in the direction normal to the fiber planes and contraction along the planes in 2D C/C structures. Post irradiation annealing above the irradiation temperature mobilizes irradiation induced defects leading to damage annealing. For the 2-D C/C structures unrecoverable damage in the form of swelling in the direction normal to the fiber planes is observed. Volumetric contraction is observed after irradiation in 3D C/C structures which is removed by post-irradiation annealing in a similar manner to the 2D C/C along the fiber planes.
- Radiolytic oxidation has a profound effect on the structural integrity of 2D and 3D C/C structures leading to exfoliation at fluences $\geq 5 \cdot 10^{20}$ p/cm²
- Tensile tests on unirradiated 3D C/C and graphite confirmed the higher strength property of the composite. Following irradiation, an increase in the E modulus is observed. Load-deflection tests using 3-point bending on irradiated 3D C/C composite revealed reduction of deflection to failure with increase in strength and E modulus as a function of dose. The tests further confirmed the negative impact of radiolytic oxidation on the mechanical strength of the composite. Load deflection studies of irradiated Mo-GRCF showed the inability of carbon fibers which do not form a mesh within the compound to offer any “yielding” leading to a totally brittle failure.
- The x-ray diffraction studies on as received and irradiated 2D C/C, 3D C/C graphite and Mo-GRCF showed that the degree of graphitization achieved varies between the matrix and the fibers in the 2D and 3D C/C with the fibers assuming the least crystallized phase. Irradiation-induced crystallization is observed at the fluence of $6 \cdot 10^{20}$ p/cm² along with a turbostratic state in the matrix. Slightly larger d_{002} spacing results in 3D C/C following irradiation to that exhibited by irradiated fine grain graphite (IG-430) with similar dose. High degree of crystallization is achieved in Mo-GRCF.
- Irradiated 3D C/C in an inert gas environment (argon) to a fluence of $6 \cdot 10^{20}$ p/cm² has shown to have increased its E modulus and consequently the strength due to pinning of dislocations by irradiation induced defects and maintained its structural integrity. Lattice c-parameter, however, experiences a change of $\sim 2.82\%$ to a value of 3.47288 (Å) which is within the regime of exfoliation of graphite.
- The Mo-GRCF irradiated to a fluence in excess of $5 \cdot 10^{20}$ p/cm², vacuum atmosphere and temperature $>400^\circ\text{C}$ has experienced structural degradation, a finding supported by the brittle fracture observed following much lower irradiation dose (0.10^{18} p/cm²).

REFERENCES

1. Tsai, S.-C., et al., Microstructural evolutions of three-dimensional carbon-carbon composite materials irradiated by carbon ions at elevated temperatures, *Progress in Nuclear Energy* (2012), doi:10.1016/j.pnucene.2011.11.010
2. T. Paulmier, et al., “Structural modifications of carbon-carbon composites under high temperature and ion irradiation,” *Applied Surface Science* 243 (2005) 376–393
3. T. D. Burchell. Irradiation Induced Structure and Property Changes in Tokamak Plasma-Facing, Carbon-Carbon Composites,” In Proc 39th SAMPE Symposium, Vol. 39, pp. 2423-2436, 1994
4. T. Nishida and H. Sueyoshi “Effects of Carbon Fiber Orientation and Graphitization on Solid State Bonding of C/C Composite to Nickel,” *Materials Transactions*, Vol. 44, No. 1 (2003) pp. 148-154
5. N. Simos, “Composite Materials under Extreme Radiation and Temperature Environments of the Next Generation Nuclear Reactors,” *Composite Materials-Book II*, Intech Publishers, ISBN 978-953-307-1098-3, 2011
6. D. G. Schweitzer, “Activation Energy for Single Interstitials in Neutron-Irradiated Graphite and the Absolute Rate of Formation of Displaced Atoms,” *Physical Review*, Vol. 128, No. 2, 1962
7. J.H. Gittus “Creep, Viscoelasticity and Creep Fracture in Solids,” Elsevier Science Ltd, 1975
8. B.T. Kelly and Brocklehurst, *Carbon* 9, 783 (1971)
9. Kelly BT. “On the amorphization of graphite under neutron irradiation,” *Journal of Nuclear Materials*, 172(2), pp.237–238, 1990
10. J-P. Bonal, et al “Graphite, Ceramics, and Ceramic Composites for High-Temperature Nuclear Power Systems,” *MRS Bulletin*, Vol. 34, pp. 28-34, 2009
11. N. Simos, et al., “Material Property Studies under Irradiation at Brookhaven National Laboratory Linear Isotope Producer,” *Physical Review Special Topics-Accelerators and Beams*, Paper No. ZY10053, 2011
12. N. Simos, et al., “Thermal Shock Induced by a 24 GeV Proton Beam in the Test Windows of the Muon Collider Experiment E951 – Test Results and Theoretical Predictions”, *Nuclear Applications in the New Millennium (AccAPP-ADDTA'01)*, 2001
13. N. Simos, et al., “Solid Target Studies for Muon Colliders and Neutrino Beams,” *Nuclear Physics B*, 155, pp. 288-290, 2006
14. N. Simos, et al., “Experimental Studies of Targets and Collimators for High Intensity Beams,” *ICFA-HB 2006*, Paper No. TUBZ04, 2006
15. N. Simos, H. Kirk, P. Thieberger, et al., *Material Studies for Pulsed, High Intensity Proton Beam Targets*, *Nuclear Physics B*, 2005
16. N. Simos, et al, “Long Baseline Neutrino Experiment (LBNE) Target Material Radiation Damage

from Energetic Protons of the Brookhaven Linear Isotope Production (BLIP) Facility,” **BNL-111826-2016-IR**

17. N. Simos, et al, “BNL Irradiation Damage Studies of the Metal Matrix Composite Mo-GRCF Considered for High Luminosity LHC Collimator,” BNL-111828-2016-IR
18. Simos, N., et al (2008). Irradiation damage studies of high power accelerator materials. *Journal of Nuclear Materials*, Vol. 377, Part 1, pp. 41-51
19. W. Bollmann. “Electron-microscopic observations on radiation damage in graphite” *Phil. Mag.*, 5(54):621{624, June 1960.
20. Snead LL, Burchell TD, Katoh Y., “Swelling of nuclear graphite and high quality carbon fiber composite, under very high irradiation temperature,” *J Nucl Mater.* 381(1–2), pp.55–61, 2008
21. N. V. Mokhov, The MARS Code System User’s Guide, Fermilab-FN-628 (1995); N. V. Mokhov, S. I. Striganov, MARS15 Overview, in Proc. of Hadronic Shower Simulation Workshop, Fermilab, Sept. 2006 AIP Conf. Proc. 896, pp. 50-60 (2007); N. V. Mokhov et al., Prog. Nucl. Sci. Technol. 4, 496 (2014); <http://dx.doi.org/10.15669/pnst.4.496>; <http://www-ap.fnal.gov/MARS/>
22. "The FLUKA Code: Developments and Challenges for High Energy and Medical Applications" T.T. Böhlen, F. Cerutti, M.P.W. Chin, A. Fassò, A. Ferrari, P.G. Ortega, A. Mairani, P.R. Sala, G. Smirnov and V. Vlachoudis, *Nuclear Data Sheets 120*, **211-214 (2014)**
23. "FLUKA: a multi-particle transport code" A. Ferrari, P.R. Sala, A. Fasso, and J. Ranft, *CERN-2005-10* (2005), INFN/TC_05/11, SLAC-R-773